sustainability

MDPI

Article

Impact of Volcanic Ash on Road and Airfield Surface Skid Resistance

Daniel M. Blake [1,*], Thomas M. Wilson [1], Jim W. Cole [1], Natalia I. Deligne [2] and Jan M. Lindsay [3]

[1] Department of Geological Sciences, University of Canterbury, Private Bag 4800, Christchurch 8041, New Zealand; thomas.wilson@canterbury.ac.nz (T.M.W.); jim.cole@canterbury.ac.nz (J.W.C.)
[2] GNS Science, 1 Fairway Drive, Avalon 5010, P.O. Box 30-368, Lower Hutt 5040, New Zealand; n.deligne@gns.cri.nz
[3] School of Environment, The University of Auckland, Private Bag 92019, Auckland 1142, New Zealand; j.lindsay@auckland.ac.nz
* Correspondence: daniel.blake@pg.canterbury.ac.nz; Tel.: +64-21-050-1450

Received: 14 July 2017; Accepted: 31 July 2017; Published: 6 August 2017

Abstract: Volcanic ash deposited on paved surfaces during volcanic eruptions often compromises skid resistance, which is a major component of safety. We adopt the British pendulum test method in laboratory conditions to investigate the skid resistance of road asphalt and airfield concrete surfaces covered by volcanic ash sourced from various locations in New Zealand. Controlled variations in ash characteristics include type, depth, wetness, particle size and soluble components. We use Stone Mastic Asphalt (SMA) for most road surface experiments but also test porous asphalt, line-painted road surfaces, and a roller screed concrete mix used for airfields. Due to their importance for skid resistance, SMA surface macrotexture and microtexture are analysed with semi-quantitative image analysis, microscopy and a standardised sand patch volumetric test, which enables determination of the relative effectiveness of different cleaning techniques. We find that SMA surfaces covered by thin deposits (~1 mm) of ash result in skid resistance values slightly lower than those observed on wet uncontaminated surfaces. At these depths, a higher relative soluble content for low-crystalline ash and a coarser particle size results in lower skid resistance. Skid resistance results for relatively thicker deposits (3–5 mm) of non-vesiculated basaltic ash are similar to those for thin deposits. There are similarities between road asphalt and airfield concrete, although there is little difference in skid resistance between bare airfield surfaces and airfield surfaces covered by 1 mm of ash. Based on our findings, we provide recommendations for maintaining road safety and effective cleaning techniques in volcanic ash environments.

Keywords: volcanic ash; asphalt; concrete; runway; highway; traction; British Pendulum Tester; safety

1. Introduction

1.1. Background

Functional transport networks are critical for society both under normal operating conditions and in emergencies. During volcanic eruptions, transport networks may be required for the evacuation of residents, to allow sufficient access for emergency services or military personnel to enter affected areas and for regular societal activities. Once direct threats have subsided, transport networks are crucial for both immediate and long-term recovery, including the clean-up and disposal of material, and restoration of services and commerce. It is thus imperative that effective and realistic transport management strategies are incorporated into volcanic contingency planning in areas where society

and infrastructure are at risk (e.g., Auckland, New Zealand; Kagoshima, Japan; Mexico City, Mexico; Naples, Italy; Yogyakarta, Indonesia).

Volcanic eruptions produce many hazards. Damage to transport from proximal hazards such as lava flows, pyroclastic density currents and lahars is often severe, leaving ground routes impassable and facilities such as airports closed or inoperable. Volcanic ash (ejected material with particle sizes <2 mm in diameter) is widely dispersed and, although not necessarily damaging to static transport infrastructure, is generally the most disruptive of all volcanic hazards [1,2]. Even relatively small eruptions are capable of widespread disruption on ground transport and aviation, which may continue for months due to the remobilisation and secondary deposition of ash by wind, traffic or other human activities, even after an eruption has subsided.

To date studies on the impacts of volcanic hazards to society have focussed on the effects of ash [2–13]. These studies and reports suggest four frequently occurring types of volcanic ash impacts on surface transport:

1. Reduction of skid resistance on roads and runways covered by volcanic ash
2. Coverage of road and airfield markings by ash
3. Reduction in visibility during initial ashfall and any ash re-suspension
4. Blockage of engine air intake filters which can lead to engine failure.

Despite much anecdotal evidence, detailed work to quantify the impact of ash on surface transport including roads and airfields is in its infancy [12,14]. Quantitative, empirical evidence can inform management strategies in syn-eruptive and post-ashfall environments such as evacuation planning, safe travel advice in the recovery phase and recommended clean-up operations.

Most studies of exposed critical infrastructure have generally focussed on very large eruptions and ashfall deposits >10 mm thick, rarely reporting the effects from ashfall <10 mm thick [10]. This presents a source of uncertainty for emergency management planning and loss assessment models, which is important, as thin deposits are more frequent and often cover larger areas [15]. Some notable eruptions that have led to reported reduced skid resistance on roads in the past are highlighted in Table 1. It has been suggested that impacts start at ~2–3 mm ash thickness [2], although there have been few studies that have quantified such impacts in detail. Indeed, the limited quantitative data available from historic observations generally relates impacts to approximate depths of ash, which may not be the best metric: ash characteristics such as particle size, ash type, degree of soluble components and wetness, may influence or even control the level of skid resistance. We investigate the importance of these alternative characteristics in this paper.

Here, we present experimental methods and results from the University of Canterbury's Volcanic Ash Testing Laboratory (VAT Lab) on the reduction of skid resistance on surfaces covered by volcanic ash. We test the skid resistance on road and airfield surfaces using the British Pendulum Tester (BPT), a standard instrument used by road engineers for surface friction testing since its development in the 1950s [16], and still used in many countries, particularly at problematic road sites. Despite the widespread and frequent use of the BPT by road engineers, we are unaware of other studies that have utilised the instrument on ash-covered surfaces. We note that other instruments are available to measure skid resistance on paved surfaces, including the Dynamic Friction Tester, GripTester, Sideways force Coefficient Routine Investigation Machine (SCRIM) and the Road Analyser and Recorder (ROAR) [16]. However, after an assessment of the literature, we decided that these would not be suitable for this study due to likely complications associated with testing surfaces covered in lose ash material by machines with fast-moving components, difficulties in obtaining enough volcanic ash to cover necessary travel paths, and/or potential damage to expensive components.

Table 1. Historical reports of reduced skid resistance following volcanic eruptions. There may be other instances described as 'general impacts to transportation' or which have not been recorded in the literature.

Volcano and Country	Year	Ash Thickness (mm)	Observations Related to Skid Resistance
St Helens, United States of America	1980	17	Ash became slick when wet [17–19]
Hudson, Chile	1991	not specified	Traction problems from ash on road [7,20]
Tavurvur and Vulcan, Papua New Guinea	1994	1000	Vehicles sunk and stuck in deep ash, although passable if hardened [21–23]
Sakurajima, Japan	1995	>1	Roads slippery [22,24]
Ruapehu, New Zealand	1995–1996	"thin"	Slippery sludge from ash-rain mix (roads closed) [22,25]
Soufrière Hills, United Kingdom (overseas territory)	1997	not specified	Rain can turn particles into a slurry of slippery mud [26]
Etna, Italy	2002	2–20	Traction problems, although damp and compacted ash easier to drive on [22]
Reventador, Ecuador	2002	2–5	Vehicles banned due to slippery surfaces [22,27]
Chaitén, Chile	2008	not specified	Reduced traction caused dam access problems [28,29]
Merapi, Indonesia	2010	not specified	Slippery roads caused accidents and increased journey times [30]
Pacaya, Guatemala	2010	20–30	Slippery roads with coarse ash [9]
Puyehue-Cordón Caulle, Chile	2011	>100	2WDs experienced traction problems (wet conditions) [31]
Shinmoedake, Japan	2011	not specified	Ladders very slippery [32]
Kelud, Indonesia	2014	1–100	Roads slippery with increased accident rate [33]
Sinabung, Indonesia	2014	80–100	Road travel impracticable in wet muddy ash [34]

1.2. Skid Resistance

Skid resistance (i.e., the force developed when a tyre that is prevented from rotating slides along a pavement surface [35]) is a fundamental component of road safety and should be managed so that it is adequate to enable safe operation [36]. Skid resistance is also essential for airfields to enable sufficient acceleration, deceleration and change in direction of aircraft on the surface [37]. It has become particularly important since the advent of turbojet aircraft with their greater weight and high landing speeds [38,39]. Skid resistance is essentially a measure of the Coefficient of Friction (CoF) obtained under standardised conditions in which the many variables are controlled so that the effects of surface characteristics can be isolated [40].

Skid resistance of surfaces changes over time, typically increasing in the first two years following pavement construction for roads due to the wearing by traffic, and rough aggregate surfaces becoming exposed, then decreasing over the remaining pavement life as aggregates become polished [41].

1.2.1. Surface Macrotexture and Microtexture

Surface friction is primarily a result of the macrotexture and microtexture of road and airfield pavements; these are thus intrinsically linked to skid resistance. As defined by the World Road Association-PIARC in 1987 [42]:

- Macrotexture defines the amplitude of pavement surface deviations with wavelengths from 0.5 to 50 mm.
- Microtexture is the amplitude of pavement surface deviations from the plane with wavelengths less than or equal to 0.5 mm, measured at the micron scale [43].

Microtexture, a property of each individual aggregate chip, contributes in particular to skid resistance for vehicles at low speed (i.e., the tyre rubber locally bonds to the surface through adhesion). Microtexture varies from harsh to polished. When a pavement is newly constructed, microtexture is particularly rough; however, once in service, microtexture changes due to the effects of traffic and weather conditions [43]. Macrotexture, the coarse texture of pavement surface aggregates, helps to reduce the potential for aquaplaning and provides skid resistance at high speeds through the effect of hysteresis (caused by the surface projections deforming the tyre) [36,40]. Typically, if the surface binder and aggregate chips have been appropriately applied, macrotexture levels should very gradually and linearly decrease over time as the aggregate surface slowly abrades [16].

1.2.2. Road Skid Resistance

The minimum recommended values of skid resistance and calculated corresponding CoFs for different sites on road networks that are measured with the BPT under typical wet conditions are shown in Table 2 and are reported in various literature sources internationally [41,44,45].

Table 2. Minimum recommended Skid Resistance Values for different road network sites, under wet conditions and measured using the British Pendulum Tester [41,44,45].

Type of Site	Minimum Recommended Skid Resistance Value	Corresponding Coefficient of Friction
Difficult sites such as: (a) Roundabouts (b) Bends with radius less than 150 m on unrestricted roads (c) Gradients, 1 in 20 or steeper, of lengths >100 m (d) Approaches to traffic lights on unrestricted roads	65.0	0.74
Motorways and heavily trafficked roads in urban areas (with >2000 vehicles per day)	55.0	0.60
All other sites	45.0	0.47

Rain, snow and ice are common hazards that compromise the quality of road surfaces [46–48] by interfering with surface macrotexture and microtexture. In 2003, Bennis and De Wit quantified how surface friction varies with time during a short rain shower following a reasonable period of no rain (Figure 1) [49]. The measured skid resistance significantly reduces immediately after rainfall and then recovers to a more typical wet skid resistance. However, the effect of individual contaminants, such as vehicle residues and atmospheric dust, on surface friction is poorly understood [16].

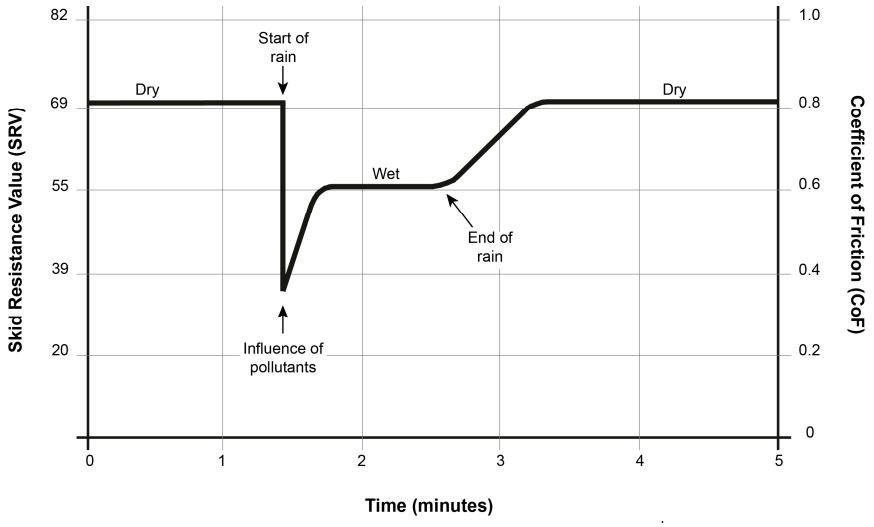

Figure 1. Variation in Coefficient of Friction (CoF) during a rain event [16,49–51].

Many studies have focused on snow- and rain-related crashes in northern states of the U.S. [52–55]. We propose that parallels may be drawn between such hazards and the hazard presented by ashfall on roads. Following a review of the literature, Aström and Wallman (2001) summarise typical CoFs for different road conditions (Table 3) [56]. The effect of hazards such as ice and snow can be substantial with most skid resistance values under such conditions falling below the minimum recommended levels (Table 2). Skid resistance is very limited under black ice conditions.

Table 3. Skid Resistance Values (SRVs) and calculated corresponding CoFs for different road conditions (adapted from [56]). The two measures of friction are related by the Equation: CoF = (3 × SRV)/(330 − SRV) [57].

Type of Site	Typical Skid Resistance Value	Corresponding Coefficient of Friction
Dry, bare surface	69.5–82.5	0.8–1.0
Wet, bare surface	62.4–69.5	0.7–0.8
Packed snow	20.6–30.0	0.20–0.30
Loose snow/slush	20.6–47.1 (higher value when tyres in contact with pavement)	0.20–0.50
Black ice	15.7–30.0	0.15–0.30
Loose snow on black ice	15.7–25.4	0.15–0.25
Wet black ice	5.4–10.6	0.05–0.10

1.2.3. Airfield Skid Resistance

In addition to the contaminants mentioned in Section 1.2.2, a common and important contaminant on airport runway surfaces is tyre rubber. With repeated aircraft landings, rubber from tyres can cover the entire surface of landing areas, filling the surface voids and reducing macrotexture and microtexture, resulting in loss of aircraft braking capacity and directional control, especially when runways are wet [38,39]. The extent of rubber tyre contaminant accumulation on runways is dependent on the volume and type of aircraft that use the airport [38].

Unfortunately, there is no common index for ground friction measurements on airfields. Currently, individual airport operating authorities are responsible for providing any take-off and landing performance data as a function of a braking coefficient with ground speed, and relating this data to a friction index measured by a ground device [58]. CoF values measured by Continuous Friction

Measuring Equipment (CFME) can be used as guidelines for evaluating friction deterioration of runway pavements [38]. The CoFs for three classification levels for Federal Aviation Administration (FAA) qualified CFME operated at 65 and 95 km h^{-1} test speeds are shown in Table 4. There are no airfield guideline thresholds for the BPT as it only provides spot friction measurements of the surface (and is not classified as CFME). However, BPTs are sometimes used on runways and we thus summarise BPT results for airfield concrete surfaces in Section 3.

Table 4. Guideline friction values for three classification levels for Federal Aviation Administration (FAA) qualified Continuous Friction Measuring Equipment (CFME) operated at 65 and 95 km h^{-1} test speeds [38]. Note that there are no airfield guideline thresholds for the British Pendulum Tester (BPT) which is not CFME and only provides spot friction measurements.

	65 km h^{-1}			95 km h^{-1}		
	Minimum	**Maintenance Planning**	**New Design/Construction**	**Minimum**	**Maintenance Planning**	**New Design/Construction**
Mu Meter	0.42	0.52	0.72	0.26	0.38	0.66
Runway Friction Tester (Dynatest Consulting, Inc.)	0.50	0.60	0.82	0.41	0.54	0.72
Skiddometer (Airport Equipment Co.)	0.50	0.60	0.82	0.34	0.47	0.74
Airport Surface Friction Tester	0.50	0.60	0.82	0.34	0.47	0.74
Safegate Friction Tester (Airport Technology USA)	0.50	0.60	0.82	0.34	0.47	0.74
Griptester Friction Meter (Findlay, Irvine, Ltd.)	0.43	0.53	0.74	0.24	0.36	0.64
Tatra Friction Tester	0.48	0.57	0.76	0.42	0.52	0.67
Norsemeter RUNAR (operated at fixed 16% slip)	0.45	0.52	0.69	0.32	0.42	0.63

1.2.4. Volcanic Ash and Skid Resistance

Due to its rapid formation, volcanic ash particles comprise various proportions of vitric (glassy, non-crystalline), crystalline or lithic (non-magmatic) particles [10] which are usually hard and highly angular. Volcanic ash properties are influenced by various factors, including the magma source type, distance from the vent, weather conditions and time since the eruption. Important volcanic ash properties include:

1. Particle size and surface area
2. Composition and degree of soluble components
3. Hardness and vesicularity
4. Angularity and abrasiveness
5. Wetness.

Since coarser and denser particles are deposited close to the source, fine glass and pumice shards are relatively enriched in ash fall deposits at distal locations [59]. Newly erupted ash has coatings of soluble components [60,61] resulting from interactions with volcanic gases and their new surfaces. Mineral fragment composition is dependent on the chemistry of the magma from which it was erupted, with the most explosive eruptions dispersing high silica rhyolite rich in hard quartz fragments [62,63]. Volcanic ash is very abrasive [3,25,64–67] with the degree of abrasiveness dependent on the hardness of the material forming the particles and their shape; high angularity leads to greater abrasiveness [10]. Most abrasion occurs from particles <500 μm in diameter, with a sharp increase in the abrasion rate from 5 to 100 μm [67].

Skid resistance from volcanic ash may be different to that expected from other contaminants due to cementitious and vesicular properties of the ash. There is also potential for large thicknesses to develop on ground surfaces or contamination to reoccur once cleaned due to re-suspension and

re-deposition. There have been several instances where road line markings have become obscured by settled volcanic ash (e.g., Mt Reventador 2002 [27], Mt Hudson 1991 [7]). An ash thickness of only ~0.1 mm can lead to road marking coverage in some cases [12]. Drivers can unintentionally drive over road markings, which may have different skid resistance properties to unmarked road surfaces. Additionally, with ash accumulation, the vibrations that drivers receive from rumble strips incorporated in some markings will likely be subdued or even eliminated, decreasing road safety further. Vehicle accidents during or after ashfall (e.g., Figure 2) are a particular concern where no road closures occur, due to decreased braking ability and increased stopping distances caused by low skid resistance.

Figure 2. Vehicle accident attributed to reduced skid resistance after ashfall from Merapi volcano, Indonesia, 2010 [68].

At airports, any observed or detected ash accumulation usually requires closure and the removal of ash from airfields before full operations can resume, both of which incur considerable expense [4]. For example, the eruption of Mt. Redoubt volcano in Alaska in 1989 resulted in a minimum loss of US $21 million at Anchorage International airport [69]. Many airports face closure even before ash settles on the airfield due to potential damage to aircraft by airborne ash, or solely the threat of ash in the vicinity. As such there are limited observations of ash resulting in reduced skid resistance on airfields, although it has been noted that slippery runways are one of the primary hazards to airports from volcanic eruptions [4].

2. Methods

2.1. Sample Preparation

2.1.1. Volcanic Ash

Volcanic ash samples derived from four different volcanic sources in New Zealand were used in this study to investigate two volcanic ash types (basalt and rhyolite) and to span a range of hardness and mineral components. The locations and ash types are shown in Table 5. Compositions and characteristics were selected as they are representative of ash likely to be encountered in the future in New Zealand, but are also common worldwide. For logistical and supply reasons, experimentation on basaltic ash was focussed on a proxy ash sourced from locally abundant basaltic lava blocks from the Lyttelton Volcanic Group at Gollans Bay Quarry in the Port Hills of Christchurch, New Zealand. Ash was physically produced from the blocks by splitting, crushing and pulverisation as described by

Broom (2010) and Wilson et al. (2012) [70,71], a method generally found to provide good correlations with real volcanic ash grain sizes. Some of the proxy Lyttelton basaltic ash produced was pulverised and sieved to 1000 µm and some to 106 µm to investigate the effect of grain size on skid resistance. In addition, further basaltic ash was sourced from deposits originating from the Pupuke eruption in the Auckland Volcanic Field and Punatekahi eruptions in the Taupo Volcanic Zone. Rhyolitic ash was sourced from deposits from the Hatepe eruption in the Taupo Volcanic Zone. These three samples were pulverised (splitting and crushing was not necessary due to their smaller original sizes) and sieved to 1000 µm (Table 5). The grain size distributions for all samples are shown in Figure 3. We note that the maximum particle sizes for all four samples sieved to 1000 µm are in fact <500 µm, likely due to the pulverisation process. Some particles for the LYT-BAS4 sample (sieved to 106 µm) exceed 106 µm due to the often-tabular nature of volcanic ash particles and their ability to pass through the sieve mesh when vertically orientated.

Table 5. Ash samples prepared for testing. Note: RCL = Ruapehu Crater Lake, WICL = White Island Crater Lake.

Ash Source	Ash Type	Sieve Size (µm)	Soluble Components Added	Sample ID
Lyttelton Volcanic Group	Hard Basalt	1000	No	LYT-BAS1
			Yes (RCL)	LYT-BAS2
			Yes (WICL)	LYT-BAS3
		106	No	LYT-BAS4
Punatekahi cone, Taupo	Scoriaceous Basalt	1000	No	PUN-BAS1
			Yes (RCL)	PUN-BAS2
			Yes (WICL)	PUN-BAS3
Hatepe ash, Taupo	Pumiceous Rhyolite	1000	No	HAT-RHY
Pupuke, Auckland Volcanic Field	Scoriaceous Basalt	1000	No	PUP-BAS1
			Yes (WICL)	PUP-BAS3

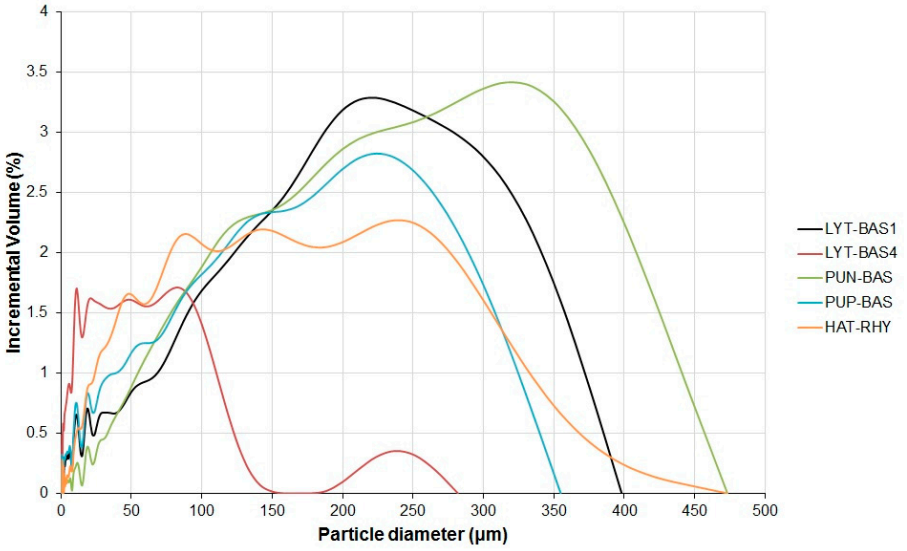

Figure 3. Mean particle size distribution analysed using a Micromeritics Saturn DigiSizer II Laser-Sizer (3× runs per sample).

As fresh ash contains adhered soluble components, we dosed a portion of our ash samples with fluid from volcanic crater lakes to mimic the volatile adsorption processes which occur in volcanic plumes, thus enabling the effects of soluble components on skid resistance to be studied. A dosing method using fluids from the crater lakes of Ruapehu and White Island volcanoes, New Zealand, described by Broom (2010) and Wilson et al. (2012) [70,71], was used for a portion of the 1000 µm

Lyttelton and Punatekahi basaltic ash samples for road testing, and Pupuke basaltic ash sample for airfield testing. The following dosing solutions were used as previous work established that they produce samples representative of real fresh volcanic ash [70,71]:

- 100% strength Ruapehu Crater Lake fluid (Table A1), i.e., no dilution, mixed at a ratio of 1:1 (ash to dosing agent)
- 20% strength White Island Crater Lake fluid (Table A1), i.e., 4 parts de-ionised water to 1 part White Island Crater Lake fluid, mixed at a ratio of 4:1 (ash to dosing agent).

We undertook a water leachate test using the method outlined by Stewart et al. (2013) [11] to measure the concentration of dissolved material in solution for all of the samples used and verify the effectiveness of dosing. Both 1:20 and 1:100 ratios of ash (g) to de-ionised water (mL) were used. The water leachate test findings (Figure A1) revealed that the soluble components in the samples we dosed (LYT-BAS2, LYT-BAS3, PUN-BAS2, PUN-BAS3, PUP-BAS3) were considerably higher than those that were not dosed and confirms that the samples used provide a suitable means of testing the effects of this characteristic on skid resistance. Additionally, the lowest pH values were generally recorded for the dosed samples.

Due to limitations in dosing fluids and possible interference caused by the crystalline characteristics of the LYT-BAS samples, most testing was undertaken using the PUN-BAS samples. Large quantities of freshly dosed ash samples were required for each thick ash test under wet conditions, hence only dry conditions were analysed for the 5 and 7 mm thick testing rounds.

2.1.2. Test Surfaces

Stone Mastic Asphalt (SMA) surfaces are commonly used on modern motorways, such as in parts of the UK and on the Auckland State Highway Network in New Zealand [72]. However, concerns have been raised about its use, as initial skid resistance may be low until the thick binder film is worn down: it sometimes takes up to two years for the material to offer an acceptable level of skid resistance [73–75]. The desire to have good macrotexture led to the development of Open Graded Porous Asphalt (OGPA) [72].

For this study, we focus mainly on tests of skid resistance for SMA surfaces using 300 × 300 × 45 mm slabs, newly constructed by the Road Science Laboratory in Tauranga, New Zealand. We also conducted some comparative tests on OGPA also constructed by the Road Science Laboratory, and on concrete surfaces constructed as 220 × 220 × 40 mm slabs by Firth Concrete. The concrete mix was compiled with the same specifications as used for placement via manual labour and a roller screed on the airfield (i.e., runways, taxiways and hardstand areas) at Auckland Airport, although we note that airfield surfaces vary between countries and airports. However, unless otherwise specified, we refer to SMA surfaces in this paper.

2.1.3. Painted Road Markings

Under typical conditions, road markings reduce accident rates [76] as they provide continuous visual guidance of features such as road edges and centres. However, when non-mechanical markings such as paint and thermoplastics are applied, the microtexture of the road surface changes and, with thicker non-mechanical markings, the macrotexture also alters as voids in the asphalt become filled. Consequently, localised skid resistance can be substantially reduced. The skid resistance of the markings is generally lower than that for the bare pavement, although the addition of retroreflective glass beads to the surface can increase skid resistance to more acceptable levels [76]. As little as 0.1 mm of volcanic ash may obscure road markings [12], meaning that drivers may unintentionally travel over marked road surfaces (e.g., such as crossing centre lines). Further accumulation may inhibit the effectiveness of rumble strips which normally cause vibrations within the vehicle.

Paint is the most common form of road marking material used in many countries, including New Zealand, and is typically applied by spraying in dry film with thicknesses varying from 70 µm to

500 µm [77]. In New Zealand, retroreflective glass beads are often applied to longitudinal centre line paint but not to paint on the road margins [78]. Road lines are usually re-painted once or twice a year to account for abrasion, with skid resistance decreasing as the paint fills more voids in the asphalt surface. With a typical asphalt lifespan of ~10 years, marking paint accumulation can be substantial in places [78]. In this study we test skid resistance on SMA slabs, machine painted by Downer Group with typical road paint (Damar Bead Lock Oil Based Paint containing 63% solids), in four forms:

- 1× application (180–200 µm thick) without retroreflective glass beads
- 1× application (180–200 µm thick) with retroreflective glass beads
- 4× applications (720–800 µm thick) without retroreflective glass beads
- 4× applications (720–800 µm thick) with retroreflective glass beads.

The asphalt with one application of paint is used to replicate markings that have been heavily abraded, whereas that with four applications mimics typical marking thickness found on New Zealand roads [78].

2.2. Skid Resistance Testing

The test procedure for the BPT (Figure 4) is standardised in the ASTM E303 (2013) method [76]. It is a dynamic pendulum impact type test, based on the energy loss occurring when a rubber slider edge is propelled across the test surface. The method is intended to correlate with the performance of a vehicle with patterned tyres braking with locked wheels on a wet road at 50 km h^{-1} [45]. Since the BPT is designed to test the skid resistance of extensive surfaces in-situ, care was taken to ensure that the instrument was stable and slabs were aligned before conducting our testing in the laboratory environment. Both 3.00″ rubber mounted TRL (55) sliders (used for road testing) and 3.00″ CEN sliders (used for airfield testing), purchased from Cooper Technology UK, were used in our study.

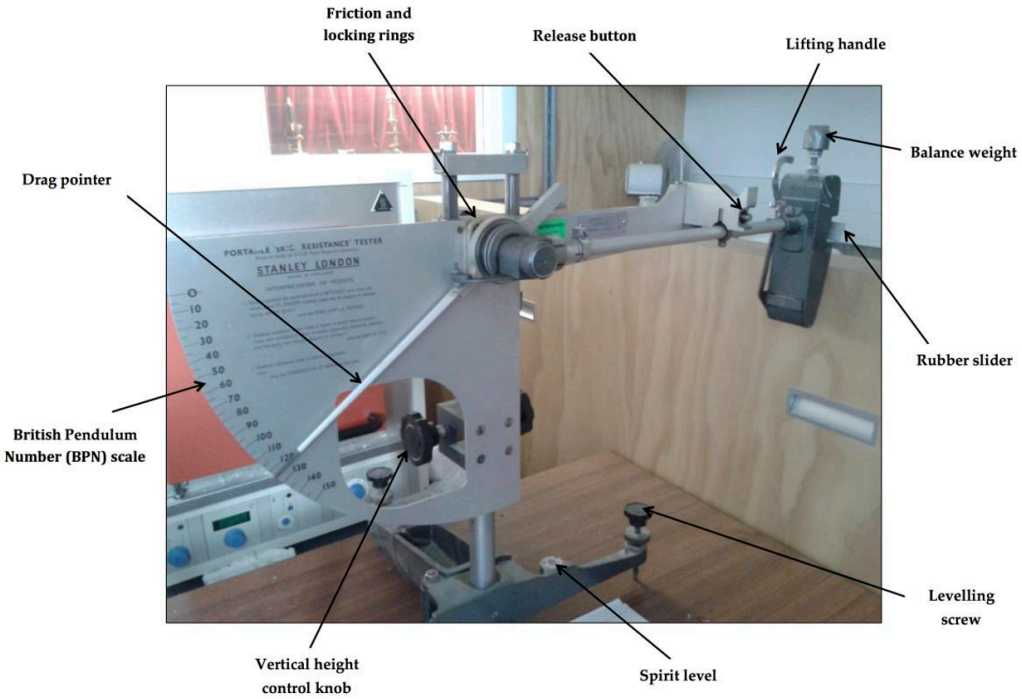

Figure 4. British Pendulum Tester (BPT) used for surface friction testing.

2.2.1. Surfaces Not Covered by Ash

As the ASTM E303 (2013) [76] method states, the direct values are measured as British Pendulum (Tester) Numbers (BPNs) [79]. Typically, tests using the BPT are conducted on wet surfaces. However,

as we are also investigating the effects of dry volcanic ash on skid resistance, we also ran the experiments under dry conditions. For surfaces not covered in ash, we adopted the same technique as used by the New Zealand Transport Agency (NZTA) [80], whereby for each test surface area, results of a minimum of five successive swings which do not differ by more than 3 BPNs are recorded. The mean of the 5 BPNs is then calculated to give a value representing skid resistance (i.e., the Skid Resistance Value (SRV)). The tests were conducted on every side of each slab to retrieve four SRVs (later averaged) for each condition. CoFs for each mean SRV are calculated using the following equation [57]:

$$\text{CoF} = (3 \times \text{SRV})/(330 - \text{SRV}) \quad (1)$$

2.2.2. Surfaces Covered by Ash

The ash characteristics analysed during experimentation and production techniques are summarised in Figure A2 [81]. For the surfaces covered in ash, we use two test methods to replicate different ash settling conditions in combination with vehicle movement effects:

1. A similar procedure as adopted by the NZTA [80] whereby five successive swings are recorded, which do not differ by more than 3 BPNs and the SRV calculated. Between each swing, ash which has been displaced by the pendulum movement is replenished with new ash of the same type (and re-wetted if applicable) to maintain a consistent depth (and wetness). This test method mimics to some degree the effect of vehicles driving during ash fall, with ash settling on a paved surface and filling any voids left by vehicle tyres before the next vehicle passes. A mean SRV is calculated by repeating the test on all four sides of each asphalt slab.
   Skid resistance was tested using 1, 3, 5 and 7 mm thick wet and dry samples on SMA, and 1, 3, 5, 7 and 9 mm thick samples on airfield concrete. Limitations in the quantity of samples prevented testing at 9 mm thick on SMA, and limitations in the quantity of rhyolite (HAT-RHY) in particular meant that testing was only conducted at 1 and 5 mm thickness on SMA for this ash type.
2. Eight successive swings of the pendulum are taken over each ash-covered test surface area but ash is not replenished between each swing. For each swing, the BPN is taken to be the SRV, allowing the change in skid resistance to be observed through analysis of the individual results. If the original surface has been wetted, further water is applied between each swing. To some degree, this method represents vehicle movement over an ash-covered surface in dry or wet conditions, where ashfall onto the road surface has ceased. A mean SRV is calculated for each successive swing by repeating the test on all four sides of each asphalt slab where possible.

In dry field conditions, the impact of remobilised ash might be more substantial than captured in the laboratory tests. However, some remobilisation during experimentation is achieved as a result of the pendulum arm movement and associated ash disturbance.

2.2.3. Cleaning

Following testing, the ash was cleaned from the asphalt concrete slabs by brushing and using compressed air if dry, or a combination of compressed air, water and light scrubbing if wet. Wetted slabs were then left to air-dry for 3–4 days before any further dry tests were conducted.

2.3. Macrotexture

2.3.1. Sand Patch Method

This volumetric technique is standardised in the ASTM E965 (2006) method [82] and summarised in Figure A3. It involves a procedure for determining the average depth of pavement macrotexture by careful application of a known volume of spherical glass beads on the surface and subsequent

measurement of the total area covered. The average pavement macrotexture depth is calculated using the following equation:

$$MTD = 4V/\pi D^2 \quad (2)$$

where MTD = mean texture depth of pavement macrotexture (mm), V = sample volume (mm^3) and D = average diameter of the area covered by the material (mm).

We use this approach to determine the macrotexture of new non-contaminated SMA surfaces and SMA surfaces that were contaminated by ash but have undergone testing (10× BPT swings) and cleaning (see Section 2.2.3). The method is not suitable for the airfield concrete slabs due to there being considerably fewer voids at the macrotexture scale and thus a much larger area would be required to conduct the test.

2.3.2. Image Analysis

In addition to the ASTM sand patch method, a visual technique involving digital photography and image analysis was adopted to distinguish between ash and asphalt at a macrotextural level on the SMA slabs. This provides a proxy for surface macrotexture and allows the relative success of cleaning techniques in relation to ash removal and skid resistance reduction to be quantitatively assessed through the calculation of remaining ash coverage. The light-coloured rhyolitic volcanic ash (sample ID: HAT-RHY) was used to allow easy visual interpretation between the ash and dark-coloured asphalt concrete.

1. White paint was marked on the edge of the slabs in order to identify the same segment of the slab between each testing round.
2. A Fuji Finepix S100 (FS) digital SLR camera (with settings: Manual, ISO 800, F6.4, 10-s timer) was mounted on a tripod directly above the asphalt slab.
3. Halogen tripod worklights were used to illuminate the surface of the slab and all ambient light was blocked out using black sheeting before images were taken to keep lighting levels consistent between photos.
4. Images were analysed for percentage coverage of ash by means of 'training' and 'segmentation' using 'Ilastik' and 'Photoshop' software.

2.4. Microtexture–Microscopy

A Meiji EMZ-8TRD (0.7–4.5 zoom) stereomicroscope and Lumenera Infinity 1 digital camera were used to capture images of 10 × 10 mm areas on the asphalt slabs and thus enable visual identification of remaining ash particles at a microtextural level. The microscope was mounted directly above the slab and Leica CLS 100 LED fibre-optic lighting was used to illuminate the Section of interest, with all ambient light blocked using black sheeting. A portable (300 × 300 mm internal dimension) grid (with 10 mm squares) was constructed to fit securely over the slab and allow easy identification of specific segments between each testing round (Figure A4).

3. Results and Discussion

3.1. Consistent Depth

When ash was replenished between each swing, the skid resistance remained relatively constant with time, permitting calculation of a mean SRV for each condition. The mean SRVs and corresponding CoFs for the non-contaminated SMA (new and cleaned) and for the SMA covered by three samples sieved to 1000 µm are shown in Figure 5. Similarly, the SRVs and CoFs for the airfield concrete, both clean and covered by two samples sieved to 1000 µm are shown in Figure 6. The Pupuke volcano sample (PUP-BAS1) was found to have very similar values to the Punatekahi (PUN-BAS1) sample. This was expected as they are both scoriaceous (highly vesiculated) basaltic rock. Due to limitations in

available ash and time constraints, full testing was only conducted with one of the scoriaceous samples on the SMA and airfield concrete.

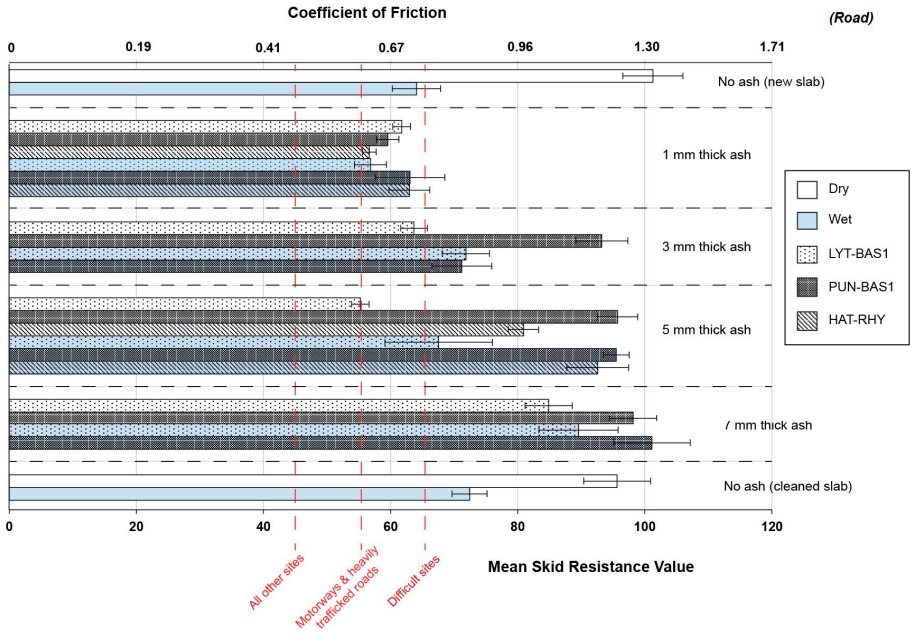

Figure 5. Mean SRVs and CoFs for the non-contaminated Stone Mastic Asphalt (SMA) and SMA covered in the three ash types sieved to 1000 µm. The error bars represent the standard deviation for each data set. Also displayed (as red dashed lines) are the minimum recommended SRVs for different road network sites (Table 2).

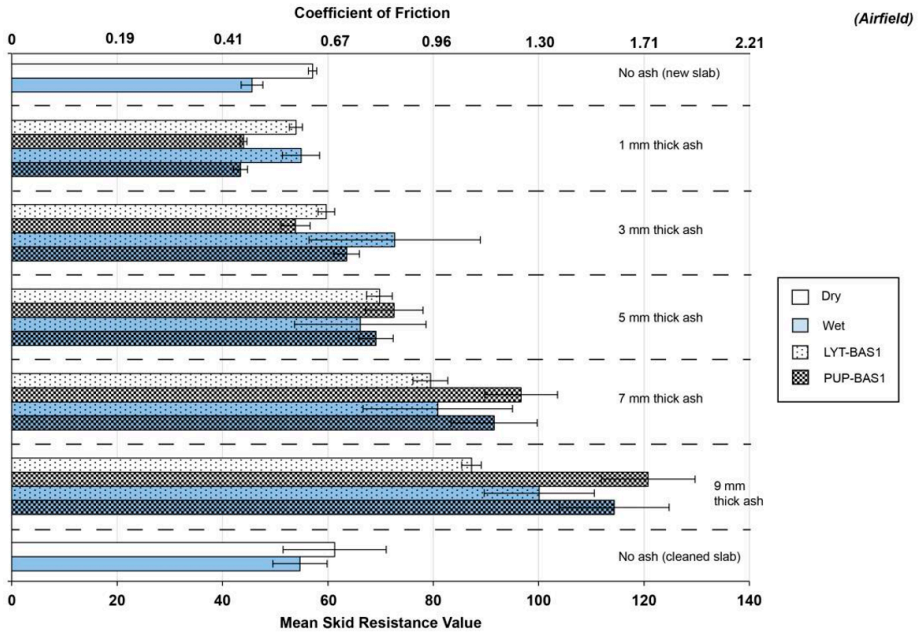

Figure 6. Mean SRVs and COFs for the non-contaminated airfield concrete and airfield concrete covered in the two ash types sieved to 1000 µm. The error bars represent the standard deviation for each data set.

3.1.1. Ash Type and Wetness

Anecdotal observations during historical eruptions suggest that skid resistance on roads is reduced following dry unconsolidated ash accumulation. This is consistent with our results, which also reveal that reduced SRVs are particularly pronounced under dry conditions for a 1 mm thick ash layer on asphalt (Figure 5). Mean SRVs for all 1 mm thick ash types fall below the minimum recommended SRV for difficult sites (an SRV of 65). Wet 1 mm ash-covered surfaces are not necessarily more slippery than dry 1 mm ash-covered surfaces and the wet surfaces covered in 1 mm thick ash are only slightly more slippery than the wet asphalt without ash contamination.

For the 3 and 5 mm thick ash-covered asphalt surfaces, we observe different trends. The LYT-BAS1 sample has similar SRVs to the 1 mm thick ash layer and the mean SRV for 5 mm is near the recommended minimum SRV for motorways (SRV 55). Samples PUN-BAS1 and HAT-RHY however, have greater SRVs than those for 1 mm of ash, suggesting that these ash types are perhaps less slippery when thicker, especially sample PUN-BAS1. The wetted PUN-BAS1 and HAT-RHY >1 mm samples have increasing SRVs as thickness increases. SRV values exceed those for bare wet asphalt surfaces and are similar to those for dry bare asphalt surfaces when ash is >5 mm thick. The vesicular nature of these two samples may play a role in increasing SRVs with the individual particles perhaps able to effectively interlock with one another and with the asphalt aggregate beneath. The pumiceous HAT-RHY sample is more friable than the PUN-BAS1 sample, which may explain the difference in mean SRVs (of up to 20) between the two. We note that the pendulum arm may be slowed upon initial impact with the thicker deposits, producing higher than true representative SRVs. However, the comparatively low SRVs for the 5 mm thick LYT-BAS1 sample suggest that other ash characteristics besides ash thickness (such as hardness and vesicularity) are also important.

Compared to asphalt, there is less difference between SRVs for bare airfield concrete surfaces and those covered by 1 mm of ash (Figure 6), perhaps due to the initially smooth surface when bare. However, as with the asphalt, results suggest little difference in slipperiness (difference in mean SRVs of <5) between wet and dry surfaces with 1 mm of ash deposition. The scoriaceous and vesicular sample PUP-BAS1 exhibits especially large SRVs as thickness is increased, reinforcing our hypothesis that ash of this type is less slippery when thicker. The apparent increase in skid resistance with the addition of ash to SRV values greater than those for bare surfaces may be a function of the pendulum arm slowing upon contact.

3.1.2. Soluble Components

There are no clear differences in SRVs observed between non-dosed and dosed LYT-BAS ash at 1 mm thick (Figure 7). However, the highly crystalline properties of this ash type may reduce the impact that dosing has on SRVs. SRVs for the dosed scoriaceous PUN-BAS ash used on road asphalt (Figure 7) and dosed scoriaceous PUP-BAS ash used on airfield concrete (Figure 8) are generally less than those which are not dosed. For all ash thicknesses, the PUN-BAS3 sample (i.e., that dosed in WICL fluid) produce mean SRVs 2-20 lower than the PUN-BAS2 sample (i.e., that dosed in RCL fluid), suggesting that the skid resistance of non-crystalline ash-covered road surfaces decreases if the soluble component of the ash increases. This corresponds with findings for other road contaminants [50], demonstrating a friction drop at the transition between no rain and rain due to the high-viscosity mix of rainwater and road debris. As such, only WICL fluid was used to dose the PUP-BAS sample (used for airfield concrete) to assess results representative of a 'likely worse-case' SRV scenario.

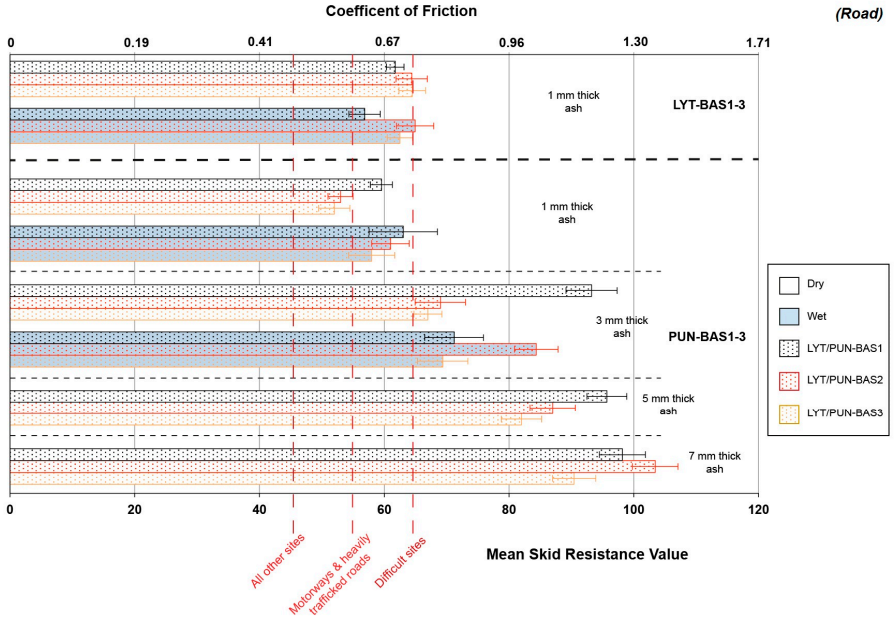

Figure 7. Mean SRVs and CoFs for the road asphalt covered in non-dosed and dosed LYT-BAS and PUN-BAS ash sieved to 1000 μm. Both samples dosed in RCL and WICL fluid under dry and wet conditions are displayed. Red dashed lines indicate the minimum recommended SRVs for different road network sites (Table 2).

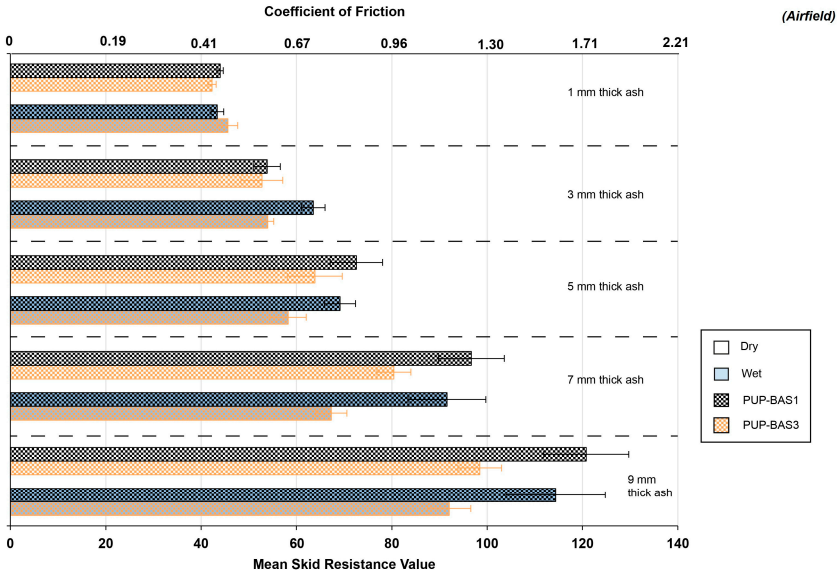

Figure 8. Mean SRVs and CoFs for the airfield concrete covered in non-dosed and dosed PUP-BAS ash sieved to 1000 μm. The samples dosed in WICL fluid under both dry and wet conditions are displayed.

3.1.3. Ash Particle Size

The mean SRVs for fine-grained basaltic ash (LYT-BAS4) are slightly higher than those for the coarse-grained ash of the same type (LYT-BAS1) when at 1 mm thickness on roads, with mean values for both wet and dry samples above the minimum recommended SRVs for difficult sites (Figure 9). This concurs with field observations made by the Kagoshima City Office staff following frequent volcanic ash deposition on roads from the multiple eruptions of Sakurajima volcano, Japan (since 1955). These observations suggest that the finer ash from the recent eruptions at the Showa crater resulted in less slippery roads than the generally coarser-grained ash produced during past eruptions from the

Minami-daki summit area [83]. We hypothesise that this difference between fine- and coarse-grained ash is due to the finer particles being more easily mobilised and displaced at the tyre-asphalt interface, allowing improved contact between the tyre and asphalt. However, no clear correlations exist between the fine- and coarse-grained ash when at 5 mm thick, perhaps due to both types covering the asphalt surface when the tyre makes contact.

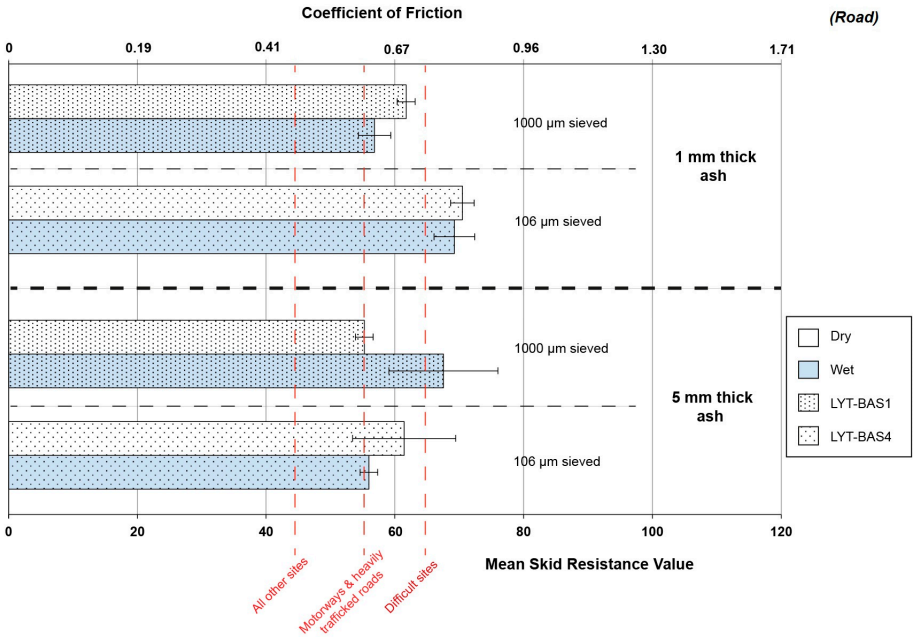

Figure 9. Mean SRVs and CoFs for the asphalt covered in coarse-grained (i.e., LYT-BAS1, 1000 µm sieved) and fine-grained (i.e., LYT-BAS4, 106 µm sieved) samples at 1 mm and 5 mm ash thickness under both dry and wet conditions. Also displayed (as red dashed lines) are the minimum recommended SRVs for different road network sites (Table 2).

3.1.4. Line-Painted Asphalt Surfaces

SRVs can be reduced substantially as a result of road markings, although the addition of retroreflective glass beads can increase values to more acceptable levels [76]. This is demonstrated in our findings for wet conditions, in which BPT analysis is typically conducted, with mean SRVs on line-painted asphalt surfaces with no beads and no ash the lowest of all our results. SRVs for these wet surfaces range from 40 to 46, and lie below the minimum recommended skid resistance for 'all other sites' when 4× coats of line paint have been applied (Figure 10). The addition of glass beads does increase SRVs (by around 5), although values are still relatively low. SRVs for 'clean' and dry line-painted asphalt surfaces are very high, but as with non-painted surfaces, the addition of a 1 mm ash layer decreases SRVs substantially. Conversely, the SRVs for wet asphalt concrete increase with a 1 mm ash layer to similar levels as for dry conditions. With the thicker (5 mm) ash layer on top of line-painted surfaces, SRVs increase further by around 20 (Figure 10).

3.1.5. Asphalt Comparison

Because of increased macrotexture of the surface, higher SRVs (~5) were measured on the bare OGPA than the SMA slabs when wet. Similar differences in SRVs existed between the two asphalt types covered by wet volcanic ash (both at 1 mm and 5 mm depths). However, no major differences in SRVs were observed between the two asphalt types when dry, whether surfaces were covered by ash or not.

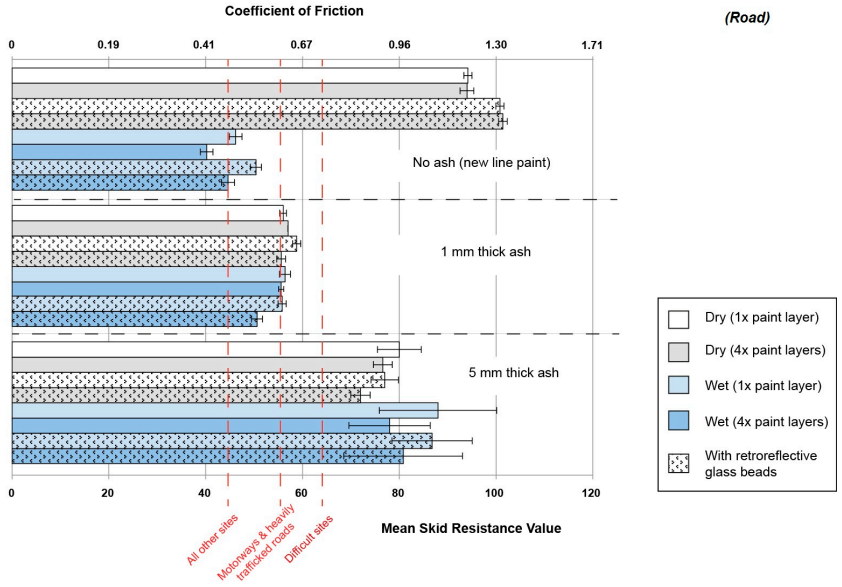

Figure 10. Mean SRVs and CoFs for the road asphalt with line-painted surfaces. Conditions of no ash, 1 mm thick ash, and 5 mm thick ash (using the LYT-BAS1 ash type) were analysed under both wet and dry conditions. Also displayed (as red dashed lines) are the minimum recommended SRVs for different road network sites (Table 2).

3.2. Inconsistent Depth

Where ash was not replenished between each swing, SRVs represent those expected for surfaces where ashfall has ceased but where there is some traffic movement.

3.2.1. Ash Types and Wetness

SRV results obtained for the samples sieved to 1000 µm (at 1 mm and 5 mm ash thickness) and deposited on road asphalt are shown in Figure 11. Note that tests of other thicknesses (3, 7 and 9 mm) were also conducted but these have been omitted from the figure for clarity.

Despite the large standard deviations, the 5 mm thick PUN-BAS1 and HAT-RHY samples initially produced high SRVs. However, the SRVs recorded for the first 2–3 swings of the pendulum over 5 mm thick ash should be interpreted with caution. This is due to possible interference of the thicker deposit when the pendulum slider first impacts the surface; similar circumstances may occur in the field when initial vehicles are driven into thicker ash deposits. When wet however, the SRVs are higher than the mean recorded on the bare asphalt surface, particularly for the PUN-BAS1 sample, suggesting that thicker layers of vesiculated (and especially harder) volcanic ash are perhaps initially less slippery than thin layers of ash of those ash types. Observations during our experimentation revealed that the wet 5 mm thick vesiculated deposits (PUN-BAS1 and HAT-RHY) consolidated, thus resisting major ash displacement more than for dry ash (Figure 12), even following several swings of the pendulum arm. The consolidated deposits were very firm to touch and, although further work is required to test this, it is suggested that light vehicles would be able to drive over the surface without sinking substantially.

Very similar patterns in skid resistance were observed for the airfield concrete surfaces where ash was not replenished between swings. The main difference was that the initially high SRVs for the scoriaceous sample (PUP-BAS) decreased more quickly with pendulum swings, most likely due to the ash being more easily displaced from the smoother concrete surface than for asphalt.

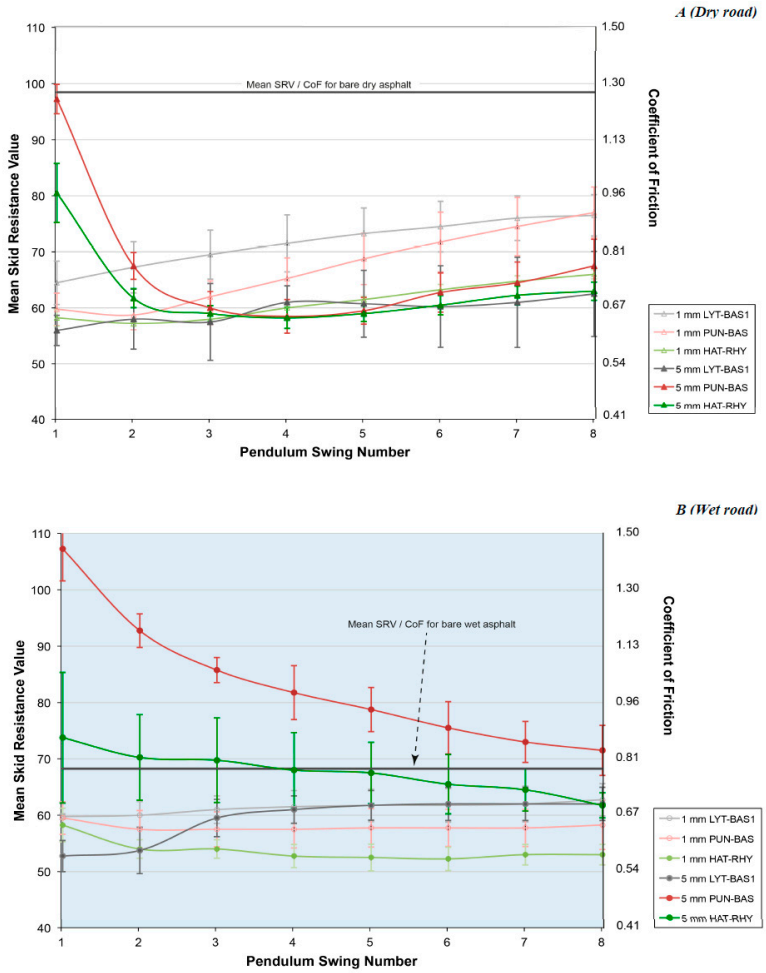

Figure 11. SRVs and corresponding CoFs on asphalt covered by ash sieved to 1000 µm, under (**A**) dry and (**B**) wet conditions. Also shown are the mean SRVs for bare asphalt, taken from Section 3.1. Error bars display the standard deviations for each pendulum swing number for the different sample types.

Figure 12. Dry ash displacement from the BPT slider-surface interface after 8× swings of the pendulum arm for (**A**) SMA and (**B**) airfield concrete. Dry ash was displaced from the surface more readily than wet ash. Note that white lines indicate length of slider contact path (i.e., 125 mm).

3.2.2. Ash Particle Size

No major changes were observed for the fine-grained basaltic ash samples (LYT-BAS4) over the course of the eight pendulum swings on asphalt, other than a gradual increase in SRVs over time, particularly for the dry ash at 1 mm thickness as observed for the coarse-grained samples (Figure 11A). As with the testing where ash was replenished, here SRVs for the fine-grained ash samples were

generally slightly higher than those for coarse-grained samples, suggesting that fine-grained ash is a little less slippery than coarser material.

3.2.3. Soluble Components

The testing involving non-replenished dosed ash confirmed the key finding already discussed during replenished testing (Section 3.1.2); non-crystalline ash containing a higher soluble component content generally produces lower SRVs than undosed ash. However, with an increasing number of swings of the pendulum, this trend becomes less pronounced, particularly under wet conditions where the effect of adding water between each test leaches the samples, thus reducing the soluble component content of the ash.

3.2.4. Line-Painted Asphalt Surfaces

Line-painted asphalt surfaces covered in ash (Figure 13) produce relatively low SRVs. Although the first 2–3 swings involving 5 mm thick ash are not considered, it is evident that wet painted surfaces are generally slightly more slippery than painted dry surfaces. The trend of quick SRV recovery (as seen in Section 3.2.1) is also evident under dry line-painted conditions, when compared to wet conditions which remain slippery for longer. Under dry conditions, the addition of retroreflective glass in the line-paint appears to aid the recovery of skid resistance over time (as shown by the rising green and orange lines for the latter swings in Figure 13A). However, this trend is not evident for wet conditions.

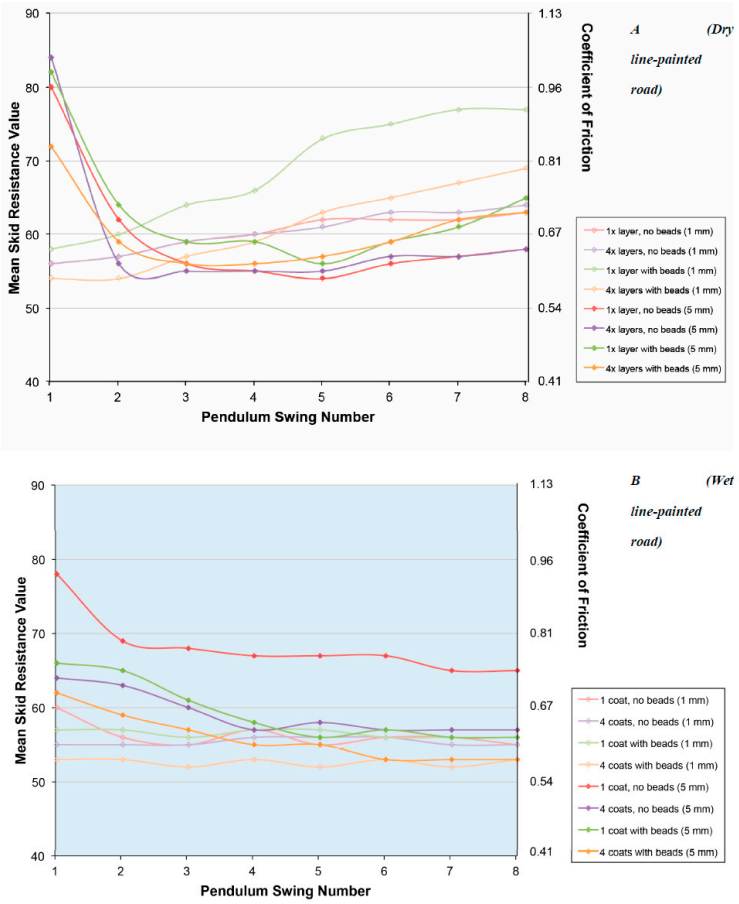

Figure 13. SRVs and corresponding CoFs for line-painted asphalt surfaces covered in 1 mm or 5 mm thick LYT-BAS1, under (**A**) dry, and (**B**) wet conditions. The initial 2–3 swings over the 5 mm deposits should be treated with caution (see text). No standard deviations are provided as only one test was conducted on each surface type due to the availability of line-painted slabs.

3.3. Surface Macro and Microtexture

3.3.1. Ash Displacement and Removal

The results for mean macrotexture depth calculated using the sand patch method for the bare, clean, new asphalt surface and the asphalt surface following dry testing and brushing, and cleaning with compressed air after contamination are shown in Table 6.

Table 6. Mean macrotexture depth of asphalt slab before and after testing/cleaning, calculated using the ASTM sand patch method, and percentage ash surface coverage.

Asphalt Concrete Slab Condition	Mean Macrotexture Depth (mm)	Ash Surface Coverage (%)
Bare, clean and new	1.37	0
Ashed, 10× BPT swings	-	81
Ashed, 10× BPT swings and brushed (10× strokes)	0.99	40
Cleaned with compressed air	1.29	<1

The results for the new slab and pre-contaminated slab after cleaning with compressed air suggest that there is little difference in macrotexture depth after cleaning using this method. However, cleaning using only brush strokes shows a mean macrotexture depth reduction of 0.38 mm, 28% less depth than the original new surface. This suggests that cleaning of dry road surfaces using only brushes may not be entirely effective and that alternative methods should be considered where possible. To confirm this, after brushing and 10× swings of the BPT, some HAT-RHY ash remains - as shown in the digital photography macrotexture image sequence (Figure 14) and semi-quantitative analysis of these images using *Ilastik* and *Adobe Photoshop* gives results of surface coverage (Table 6).

Cleaning using high-pressure water spraying and brushing was more effective than brushing alone at removing ash (<1% surface ash coverage afterwards). However, this approach requires large quantities of water and the microscope imagery revealed that some small particles of ash remain on the surface, which would perhaps still reduce skid resistance somewhat. Field observations from Kagoshima, Japan, where high quantities of only low-pressure water are used to clean road surfaces indicates that some ash remains on the road surfaces even immediately after cleaning [83]. Furthermore, clearing ash from roads using water may cause some drainage systems to become blocked [22], potentially resulting in surface water flooding.

3.3.2. Temporal Change of Skid Resistance on Bare Asphalt Surfaces

In normal conditions, the skid resistance of bare asphalt surfaces changes over time [41]. The initial trend of increasing skid resistance was confirmed during our testing of the bare wet asphalt and concrete slabs before and after contamination with ash (but following cleaning), particularly so for the asphalt (Figure 5). We suggest that the abrasive properties of volcanic ash accelerates these processes, especially for our testing as all ash particles were <500 μm in diameter (see Section 1.2.4). Following testing, the SRV of bare wet asphalt had increased by around 5. The microscopy imagery showed that the lustrous film on the new asphalt slabs had been removed during BPT experimentation (Figure 15).

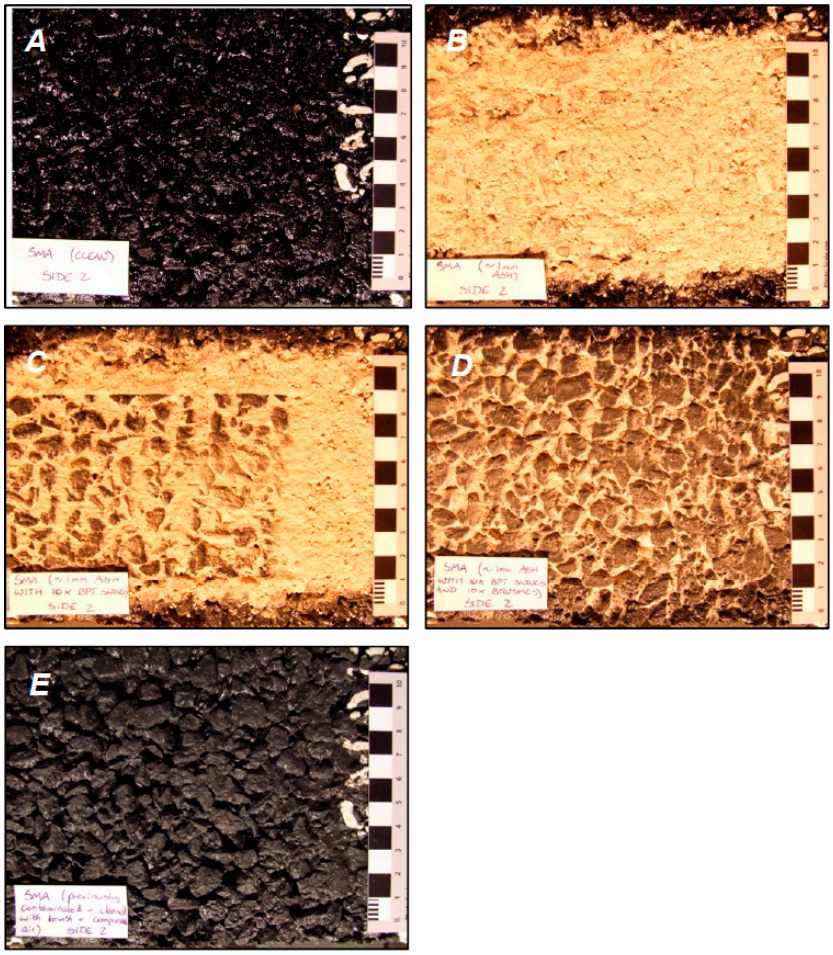

Figure 14. Macrotexture image sequence for asphalt. (**A**) Clean new slab; (**B**) covered with 1 mm rhyolitic ash (100% surface coverage); (**C**) after 10× BPT swings (81% surface ash coverage); (**D**) after cleaning with 10× brush strokes (40% surface ash coverage); (**E**) after cleaning with compressed air (<1% surface ash coverage). The macrotexture of the surface is visibly affected in images **B**–**D** with much ash remaining between the asphalt's aggregate pore spaces, even after 10× BPT swings and cleaning using a brush.

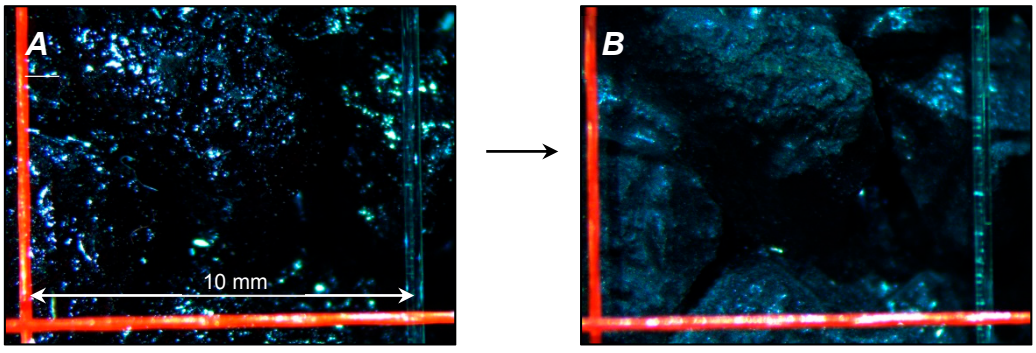

Figure 15. Microscope images on the same segment of asphalt, (**A**) on the new slab and (**B**) after contamination with volcanic ash and cleaning with compressed air. Much of the shiny film visible on the surface of the new asphalt has been removed. Note that the length of the white lines is 10 mm and that lighting conditions and microscope settings were consistent for both images.

4. Conclusions

4.1. Key Findings

Our experiments suggest that the following lead to particularly reduced skid resistance on asphalt road surfaces and may thus lead to slippery surfaces following volcanic ashfall:

- Thin (~1 mm deep) layers of relatively coarse-grained ash, with ash type having little effect at this depth (average SRVs of 55–65).
- Thicker (~5 mm deep) layers of hard, non-vesiculated ash (average SRVs of 55–60).
- Ash of low crystallinity or containing a high degree of soluble components (average SRVs ~5 lower than for ash that has undergone substantial leaching).
- Line-painted surfaces that are either dry or wet but covered by thin layers of ash, particularly when paint does not incorporate retroreflective glass beads (average SRVs of ~55).

Importantly, the largest change in skid resistance for surfaces that became covered by ash occurs during dry conditions, where SRVs fall to levels just below those for wet non-contaminated surfaces, with similar SRVs as the wet contaminated surfaces. This large reduction in skid resistance may not be expected by motorists who may consequently not adjust driving, potentially resulting in high accident rates. As time goes on, wet ash deposits on roads are most likely to lead to reduced skid resistance, particularly for thicker deposits as these remain slippery for longer (typical SRVs of around 55).

Similarities exist for airfield surfaces and the second and third bullet points above are especially true for the concrete surface type. The following additional key findings are also drawn:

- There is little difference in skid resistance between bare airfield surfaces and those covered by ~1 mm of ash.
- Low crystalline ash containing high soluble components may result in SRVs of up to 20 less than non-dosed samples, particularly if the ash is thicker (~7–9 mm depth).
- Ash is more readily displaced on smoother airfield concrete than road asphalt causing SRVs to recover to 'typical non-contaminated' values at a faster rate with consistent traffic flow.

4.2. Recommendations for Road Safety

Based on skid resistance analysis, we make the following recommendations to increase road safety in areas with volcanic ashfall exposure of $\leq$5 mm depth:

- During initial ash fall, vehicle speed (or advisory speed) should immediately be reduced to levels below those advised for driving in very wet conditions on that road, whether the surface is wet or dry. Wet ash is not necessarily more slippery than dry ash, at least initially.
- Fresh ash contains more soluble components, which results in lower skid resistance values than for leached ash. Therefore, it is important to advise motorists promptly of any restrictions.
- Particular caution should be taken on dry surfaces that become covered by coarse-grained ash as skid resistance will reduce substantially from what occurs on dry non-contaminated surfaces. The slipperiness of dry surfaces with such contamination may not be expected by motorists (skid resistance values will be similar as for wet fresh ash and slightly less than for wet non-contaminated conditions).
- Road markings may be hidden from view, impacting road safety through lack of visual and audio guidance of road features. Areas of road that are line-painted and covered in thin ash are especially slippery. Motorcyclists and cyclists in particular should take extreme care.

It is unlikely that road closures will be necessary for thin ash accumulations based on loss of skid resistance alone. SRVs rarely fall below the minimum recommended threshold for motorways and heavily trafficked roads (i.e., SRV 55) although many values fall between this and the threshold for minimum

recommended skid resistance for difficult sites (i.e., SRV 65). These results are conservative however, because of the typical reduction in skid resistance over the later stages of the pavement life. Based on observations from previous eruptions and field studies [22], physical obstruction to road vehicles may occur once ash deposits reach ~100 mm and road closures may be necessary at and above this depth. It should be stressed however, that all recommendations given ignore other impacts from volcanic ashfall such as visibility impairment, local road authority decisions, breakdowns and driver behaviour which often introduce further complexities associated with driving in volcanic ashfall. For example, lower thresholds for road closures and lower speed restrictions may be required where visibility is reduced.

4.3. Airport Safety

We do not make any specific recommendations for airport safety related to concrete airfield surfaces, although it is highlighted that extensive efforts may be required to clean airfield surfaces as has occurred following historical eruptions (e.g., Chaitén 2008 [29], Kelud 2014 [33]). It is likely that airports will remain closed until all ash has been cleared from runways due to other potential impacts such as damage to aircraft turbine engines. Our results suggest that residual ash of minimal depths on concrete airfield surfaces is likely to have little effect on skid resistance. However, airport managers should be aware that freshly erupted ash or ash that has not been leached (i.e., containing higher soluble components) will likely be more slippery than that which has persisted in the environment for some time. As with road asphalt, wet ash is not necessarily more slippery than dry ash on airfield concrete and any restrictions implemented should thus be in place for both conditions.

4.4. Recommendations for Cleaning

The following advice for road cleaning is given based on our studies of macrotexture and microtexture and from the observations during small-scale cleaning conducted on our slabs between skid resistance tests:

- Brushing alone will not restore surfaces to their original condition in terms of skid resistance. Following simple brushing practices on asphalt roads, the macrotexture depth may be around one third less than the original depth and ~40% ash coverage may occur on the surface.
- If surfaces are dry and contaminated with dry ash, air blasting combined with suction and capture of loosened ash, is an effective way to remove ash from macrotextural pores. Minor quantities of ash may remain at the microtextural level although this is deemed too low to substantially affect skid resistance.
- If surfaces are wet, a combination of water spraying and brushing and/or air blasting (with suction and ash capture) is an effective way to remove most ash and restore surface skid resistance. However, large quantities of water are required and some ash will remain in the asphalt pore spaces, especially if low-pressure water is used. Care should be taken if using water for ash removal due to the potential for blockage of some drainage systems.

Ash remobilisation should be carefully considered prior to cleaning. Extensive (and often expensive) cleaning efforts may be useless if ash continues to fall or is remobilised from elsewhere and deposited onto roads and airfields.

Acknowledgments: We thank the University of Canterbury Mason Trust scheme, New Zealand Earthquake Commission (EQC), Determining Volcanic Risk in Auckland (DEVORA) project, Natural Hazard Research Platform (research contract: C05X0907), and GNS Science for their support towards the study through the provision of funding to researchers. We also express thanks to the organisations and people who helped source equipment that was vital to the project. In particular, we would like to thank Alan Nicholson and John Kooloos of the Civil and Natural Resources Engineering department at the University of Canterbury for the loan of the BPT, and Janet Jackson, Howard Jamison and the wider laboratory and road teams at Downer Group for their support towards coordinating the construction and line-painting of asphalt slabs and for providing Daniel Blake with BPT training. We thank Roy Robertson (Auckland Airport) and Robert McKinnon (Firth Concrete) for their advice on airfield surfaces and for providing the airfield concrete slabs used in this study. Particular thanks also go to the

people who provided support with the laboratory set-up at various stages, including technician support from Rob Spiers, Matt Cockcroft, Chris Grimshaw and Sacha Baldwin-Cunningham. We also thank researchers Emily Lambie, Rinze Schuurmans, Alec Wild and Alistair Davies for their assistance with sample preparation and skid resistance testing.

Author Contributions: All authors contributed to the manuscript. D.M.B. conducted the majority of the planning, research and laboratory testing, and also led the writing and editing of the article. T.M.W. assisted D.M.B. in the development of the methodology including potential experimental approaches. T.M.W., J.W.C., N.I.D. and J.M.L. conducted multiple reviews of the article prior to submission.

Conflicts of Interest: The authors declare no conflicts of interest.

Appendix A

Table A1. Concentration of elements in the Ruapehu and White Island Crater Lake fluids at the strength used to dose the ash (after Broom 2010, Wilson 2012 [70,71]).

Element	Concentration (mg/L)	
	Ruapehu Crater Lake (100% Strength)	White Island Crater Lake (20% Strength)
Aluminium (Al)	370	965
Boron (B)	17.2	28.6
Bromine (Br)	10.8	44.2
Calcium (Ca)	909	823
Chlorine (Cl)	5568	19,452
Fluorine (F)	133	1518
Iron (Fe)	424	179
Potassium (K)	90	686
Lithium (Li)	0.77	5.60
Magnesium (Mg)	1067	1325
Sodium (Na)	660	3372
Ammonia (NH_3)	13.0	24.8
Sulphate (SO_4^{2-})	7988	4952
pH	**1.13**	**0.07**

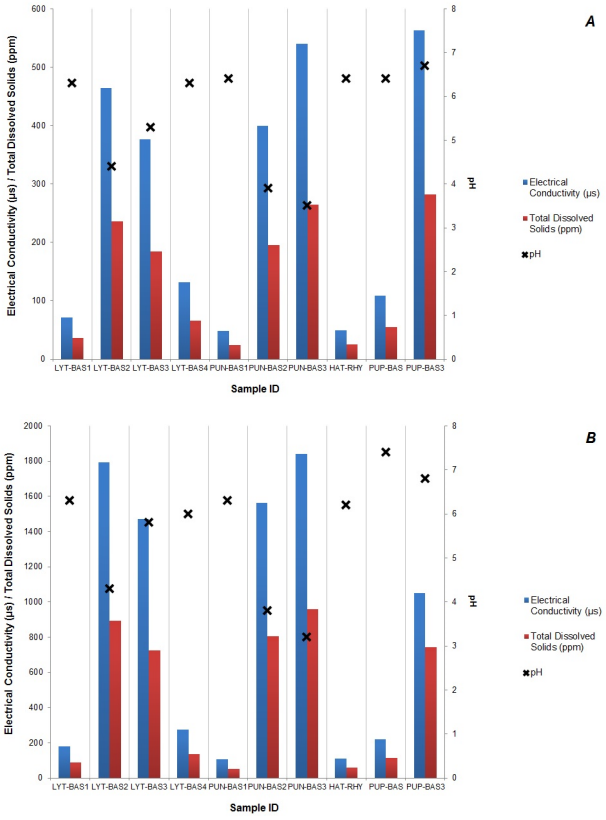

Figure A1. Water leachate results showing relative soluble components (expressed as Electrical Conductivity (EC) and Total Dissolved Solids (TDS)), and pH. (**A**) 1:100 ash to de-ionised water; (**B**) 1:20 ash to de-ionised water.

Chracteristic	Variables	Method Summary
Ash type	Hard basalt, scoriaceous basalt, pumiceous rhyolite	Different volcano source locations in New Zealand
Ash grain size	<1000 µm, <106 µm	Rock splitting, crushing and pulverisation (as required), then sieving
Ash thickness	1-2 mm, 5 mm	Manual sprinkling (1-2 mm), Metal spacer across ash surface (5 mm)
Soluble components	Non-dosed, dosed with Ruapehu Crater Lake fluid, dosed with White Island Crater Lake fluid	Established laboratory dosing technique (see section 2.1.1)
Wetness	Wetted to saturation, dry (no added moisture)	Hand-held water sprayer (water at room temperature)

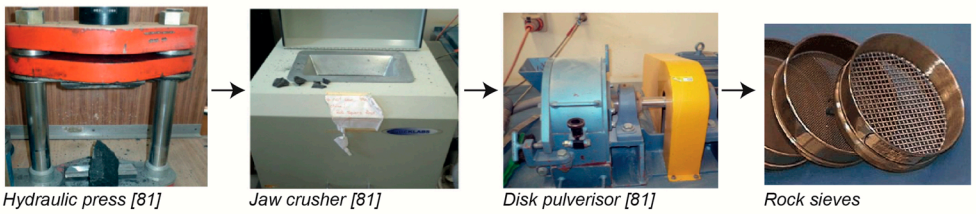

Hydraulic press [81] *Jaw crusher [81]* *Disk pulverisor [81]* *Rock sieves*

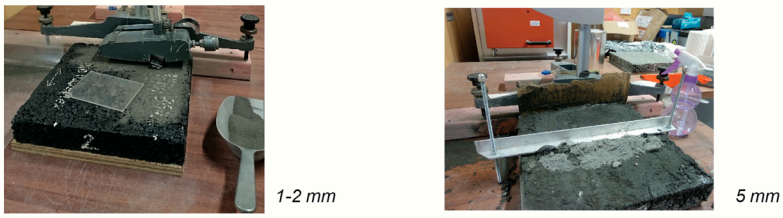

1-2 mm *5 mm*

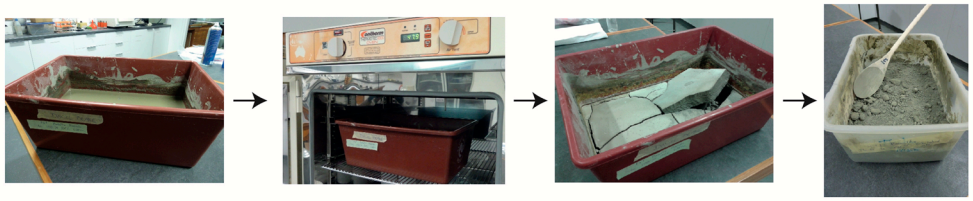

Dry *Wet*

Figure A2. Ash characteristics analysed during experimentation and illustrations to show production of each characteristic.

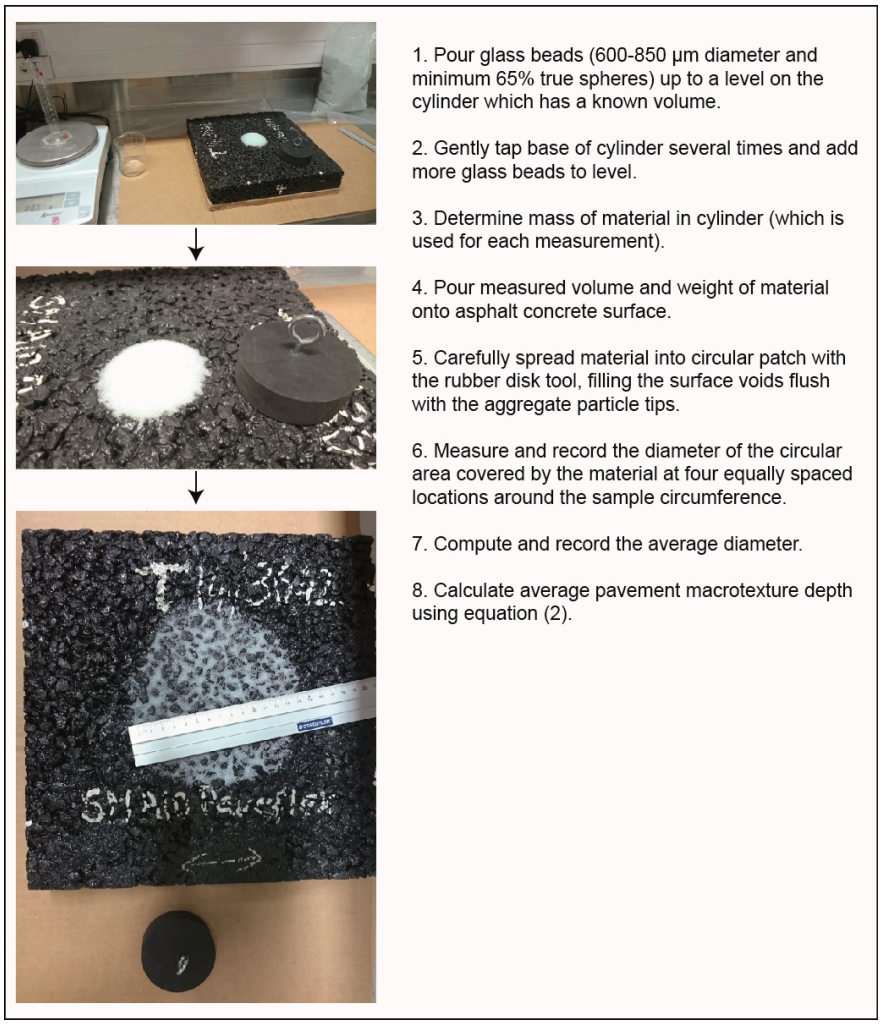

Figure A3. Summary of sand patch volumetric technique used to calculate the average pavement macrotexture depth (adapted from [82]).

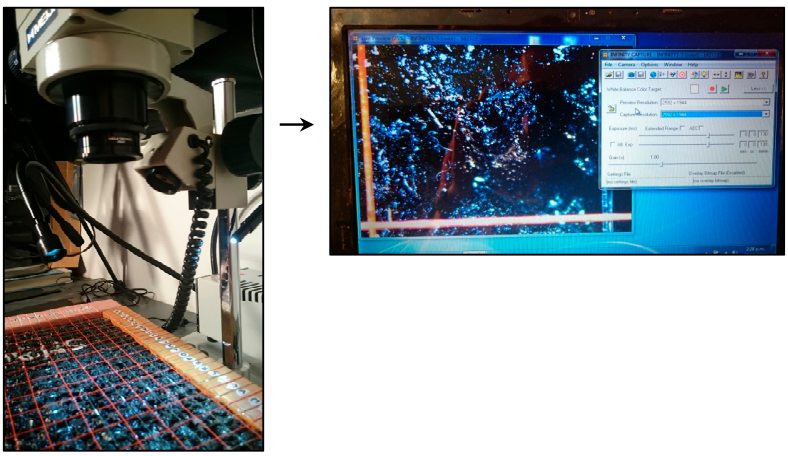

Figure A4. Image capture using stereo-microscope to analyse asphalt at a microtextural scale. Note that the grid squares are spaced at 10 mm intervals.

References

1. Johnston, D.M.; Daly, M. Auckland erupts!! *N. Z. Sci. Mon.* **1995**, *8*, 6–7.
2. Wilson, G.; Wilson, T.M.; Deligne, N.I.; Cole, J.W. Volcanic hazard impacts to critical infrastructure: A review. *J. Volcanol. Geotherm. Res.* **2014**, *286*, 148–182. [CrossRef]
3. Blong, R.J. *Volcanic Hazards: A Sourcebook on the Effects of Eruptions*; Academic Press Inc.: Sydney, Australia, 1984.
4. Guffanti, M.; Mayberry, G.C.; Casadevall, T.J.; Wunderman, R. Volcanic hazards to airports. *Nat. Hazards* **2009**, *51*, 287–302. [CrossRef]
5. Wilson, T.; Daly, M.; Johnston, D. *Review of Impacts of Volcanic Ash on Electricity Distribution Systems, Broadcasting and Communication Networks*; Technical Publication No. 051; Auckland Engineering Lifelines Group, Auckland Regional Council: Auckland, New Zealand, 2009.
6. Horwell, C.J.; Baxter, P.J.; Hillman, S.E.; Damby, D.E.; Delmelle, P.; Donaldson, K.; Dunster, C.; Calkins, J.A.; Fubini, B.; Hoskuldsson, A.; et al. *Respiratory Health Hazard Assessment of Ash from the 2010 Eruption of Eyjafjallajökull Volcano, Iceland: A Summary of Initial Findings from a Multi-Centre Laboratory Study*; International Volcanic Health Hazard Network (IVHHN), Durham University: Durham, UK, 2009.
7. Wilson, T.M.; Stewart, C.; Cole, J.W.; Dewar, D.J.; Johnston, D.M.; Cronin, S.J. *The 1991 Eruption of Volcan Hudson, Chile: Impacts on Agriculture and Rural Communities and Long-Term Recovery*; GNS Science Report 2009/66; GNS Science: Lower Hutt, New Zealand, 2011; p. 77.
8. Dunn, M.G. Operation of gas turbine engines in an environment contaminated with volcanic ash. *J. Turbomach.* **2012**, *134*, 051001. [CrossRef]
9. Wardman, J.; Sword-Daniels, V.; Stewart, C.; Wilson, T. *Impact Assessment of the May 2010 Eruption of Pacaya Volcano, Guatemala*; GNS Science Report 2012/09; GNS Science: Lower Hutt, New Zealand, 2012.
10. Wilson, T.M.; Stewart, C.; Sword-Daniels, V.; Leonard, G.S.; Johnston, D.M.; Cole, J.W.; Wardman, J.; Wilson, G.; Barnard, S.T. Volcanic ash impacts to critical infrastructure. *Phys. Chem. Earth* **2012**, *45–46*, 5–23. [CrossRef]
11. Stewart, C.; Horwell, C.; Plumlee, G.; Cronin, S.; Delmelle, P.; Baxter, P.; Calkins, J.; Damby, D.; Mormon, S.; Oppenheimer, C. Protocol for Analysis of Volcanic Ash Samples for Assessment of Hazards from Leachable Elements. Available online: http://www.ivhhn.org/images/pdf/volcanic_ash_leachate_protocols.pdf (accessed on 2 August 2017).
12. Blake, D.M.; Wilson, T.M.; Gomez, C. Road marking coverage by volcanic ash. *Environ. Earth Sci.* **2016**, *75*, 1–12. [CrossRef]
13. Hayes, J.; Wilson, T.M.; Deligne, N.I.; Cole, J.; Hughes, M. A model to assess tephra clean-up requirements in urban environments. *J. Appl. Volcanol.* **2017**, *6*. [CrossRef]
14. Blake, D.M.; Wilson, T.M.; Stewart, C. Visibility in airborne volcanic ash: Considerations for surface transportation using a laboratory-based method. *Nat. Hazards*. in review.
15. Pyle, D.M. The thickness, volume and grainsize of tephra fall deposits. *Bull. Volcanol.* **1989**, *51*, 1–15. [CrossRef]
16. Wilson, D.J. An Analysis of the Seasonal and Short-Term Variation of Road Pavement Skid Resistance. Ph.D. Thesis, Department of Civil and Environmental Engineering, University of Auckland, Auckland, New Zealand, 2006.
17. Warrick, R.A. *Four Communities under Ash*; Institute of Behavioural Science, University of Colorado: Boulder, CO, USA, 1981.
18. Cole, J.; Blumenthal, E. Evacuate: What an evacuation order given because of a pending volcanic eruption could mean to residents of the Bay of Plenty. *Tephra* **2004**, *21*, 46–52.
19. Cole, J.W.; Sabel, C.E.; Blumenthal, E.; Finnis, K.; Dantas, A.; Barnard, B.; Johnston, D.M. GIS-based emergency and evacuation planning for volcanic hazards in New Zealand. *Bull. N. Z. Soc. Earthq. Eng.* **2005**, *38*, 149–164.
20. Wilson, T.M. *Unpublished Field Notes from the Hudson Eruption Field Visit*; University of Canterbury: Christchurch, New Zealand, 2009.
21. Nairn, I.A. *The Effects of Volcanic Ash Fall (Tephra) on Road and Airport Surfaces*; GNS Science Report 2002/13; GNS Science: Lower Hutt, New Zealand, 2002; p. 32.

22. Barnard, S. The Vulnerability of New Zealand Lifelines Infrastructure to Ashfall. Ph.D. Thesis, Hazard and Disaster Management, University of Canterbury, Christchurch, New Zealand, 2009.
23. Stammers, S.A.A. The Effects of Major Eruptions of Mt Pinatubo, Philippines and Rabaul Caldera, Papua New Guinea, and the Subsequent Social Disruption and Urban Recovery: Lessons for the Future. Master's Thesis, University of Canterbury, New Zealand, 2000.
24. Durand, M.; Gordon, K.; Johnston, D.; Lorden, R.; Poirot, T.; Scott, J.; Shephard, B. *Impacts and Responses to Ashfall in Kagoshima from Sakurajima Volcano—Lessons for New Zealand*; GNS Science Report 2001/30; GNS Science: Lower Hutt, New Zealand, 2001; p. 53.
25. Johnston, D.M. Physical and Social Impacts of Past and Future Volcanic Eruptions in New Zealand. Ph.D. Thesis, Massey University, Palmerston North, New Zealand, 1997.
26. Small Explosion Produces Light Ash Fall at Soufriere Hills Volcano, Montserrat. United States Geological Survey. Available online: https://volcanoes.usgs.gov/ash/ashfall.html#eyewitness (accessed on 20 October 2015).
27. Leonard, G.S.; Johnston, D.M.; Williams, S.; Cole, J.W.; Finnis, K.; Barnard, S. *Impacts and Management of Recent Volcanic Eruptions in Ecuador: Lessons for New Zealand*; GNS Science Report 2005/20; GNS Science: Lower Hutt, New Zealand, 2006.
28. Wilson, T.M.; Cole, J.; Johnston, D.; Cronin, S.; Stewart, C.; Dantas, A. Short- and long-term evacuation of people and livestock during a volcanic crisis: Lessons from the 1991 eruption of Volcán Hudson, Chile. *J. Appl. Volcanol.* **2012**, *1*, 1–11. [CrossRef]
29. Wilson, T.M. *Unpublished Field Notes from the Chaitén Eruption Field Visit*; University of Canterbury: Christchurch, New Zealand, 2008.
30. Jamaludin, D. BORDA Respond to Merapi Disaster. Bremen Overseas Research and Development Association, South East Asia, 2010. Available online: http://www.borda-sea.org/news/borda-sea-news/article/borda-respond-to-merapi-disaster.html (accessed on 20 October 2015).
31. Wilson, T.; Outes, V.; Stewart, C.; Villarosa, G.; Bickerton, H.; Rovere, E.; Baxter, P. *Impacts of the June 2011 Puyehue-Cordón Caulle Volcanic Complex Eruption on Urban Infrastructure, Agriculture and Public Health*; GNS Science Report 2012/20; GNS Science: Lower Hutt, New Zealand, 2013; p. 88.
32. Wilson, T.M. *Unpublished Field Notes from the Shinmoedake Eruption Field Visit*; University of Canterbury: Christchurch, New Zealand, 2011.
33. Blake, D.M.; Wilson, G.; Stewart, C.; Craig, H.M.; Hayes, J.L.; Jenkins, S.F.; Wilson, T.M.; Horwell, C.J.; Andreastuti, S.; Daniswara, R.; et al. *The 2014 Eruption of Kelud Volcano, Indonesia: Impacts on Infrastructure, Utilities, Agriculture and Health*; GNS Science Report 2015/15; GNS Science: Lower Hutt, New Zealand, 2015; p. 139.
34. The Sub-Plinan Eruption of Mt Kelut Volcano on 13 Feb 2014. *Volcano Discovery*. 2014. Available online: http://www.volcanodiscovery.com/kelut/eruptions/13feb2014plinian-explosion.html (accessed on 31 October 2016).
35. Highway Research Board. *National Cooperative Highway Research Program Synthesis of Highway Practice 14: Skid Resistance*; National Academy of Sciences: Washington, DC, USA, 1972.
36. Dookeeram, V.; Nataadmadja, A.D.; Wilson, D.J.; Black, P.M. The skid resistance performance of different New Zealand aggregate types. In Proceedings of the IPENZ Transportation Group Conference, Shed 6, Wellington, New Zealand, 23–26 March 2014.
37. International Civil Aviation Organisation, Regional Aviation Safety Group (Asian and Pacific Region). Industry Best Practices Manual for Timely and Accurate Reporting of Runway Surface Conditions by ATS/AIS to Flight Crew. 2013. Available online: http://www.icao.int/APAC/Documents/edocs/FS-07IBP%20Manual%20on%20Reporting%20of%20Runway%20Surface%20Condition.pdf (accessed on 2 October 2015).
38. U.S. Department of Transportation, Federal Aviation Administration. Measurement, Construction and Maintenance of Skid-Resistant Airport Pavement Surfaces. Advisory Circular 150/5320-12C. 1997. Available online: http://www.faa.gov/documentLibrary/media/advisory_circular/150-5320-12C/150_5320_12c.PDF (accessed on 3 October 2015).
39. Airport Runways: Skid Resistance and Rubber Removal. *Blastrac*. 2015. Available online: http://pdf.aeroexpo.online/pdf/blastrac/airport-runways-skid-resistance-rubber-removal/168551-3763.html (accessed on 2 August 2017).
40. Wilson, D.J.; Chan, W. *The Effects of Road Roughness (and Test Speed) on GripTester Measurements*; New Zealand Transport Agency Research Report 523; Clearway Consulting Ltd.: Auckland, New Zealand, 2013.
41. Asi, I. Evaluating skid resistance of different asphalt concrete mixes. *Build. Environ.* **2007**, *42*, 325–329. [CrossRef]

42. World Road Association-PIARC. Technical committee report on road surface characteristics, Permanent International Association of Road Congress. In Proceedings of the 18th World Congress, Brussels, Belgium, 13–19 September 1987.
43. Ergun, M.; Iyinam, S.; Iyinam, F. Prediction of road surface friction coefficient using only macro- and microtexture measurements. *J. Transp. Eng.* **2005**, *131*, 311–319. [CrossRef]
44. Manual, B.P. *Operation Manual of the British Pendulum Skid Resistance Tester*; Wessex Engineering Ltd.: Victoria, BC, Canada, 2000.
45. Skid Tester: AG190. Impact Test Equipment Ltd. Available online: http://www.impact-test.co.uk/docs/AG190_HB.pdf (accessed on 4 November 2014).
46. Benedetto, J. A decision support system for the safety of airport runways: The case of heavy rainstorms. *Transp. Res. Part A Policy Pract.* **2002**, *8*, 665–682. [CrossRef]
47. Andrey, J. Relationships between weather and traffic safety: Past, present and future directions. *Climatol. Bull.* **1990**, *24*, 124–136.
48. Cova, T.; Conger, S. Transportation hazards. In *Transportation Engineers' Handbook*; Kutz, M., Ed.; Centre for Natural and Technological Hazards, University of Utah: Salt Lake City, UT, USA, 2003.
49. Bennis, T.A.; De Wit, L.B. PIARC State-of-the-Art on Friction and IFI. In Proceedings of the 1st Annual Australian Runway and Roads Friction Testing Workshop, Sydney, Australia, 5 August 2003.
50. Persson, B.N.J.; Tartaglino, U.; Albohr, O. Rubber friction on wet and dry road surfaces: The sealing effect. *Phys. Rev. B* **2005**, *71*, 035428. [CrossRef]
51. Do, M.T.; Cerezo, V.; Zahouani, H. Laboratory test to evaluate the effect of contaminants on road skid resistance. *Proc. Inst. Mech. Eng. Part J J. Eng. Tribol.* **2014**, *228*, 1276–1284. [CrossRef]
52. Qin, X.; Noyce, D.; Lee, C.; Kinar, J.R. Snowstorm event-based crash analysis. *Transp. Res. Rec.* **2006**, *1948*, 135–141. [CrossRef]
53. Khattak, A.J.; Knapp, K.K. Interstate highway crash injuries during winter snow and non-snow events. *Transp. Res. Board* **2001**, *1746*, 30–36. [CrossRef]
54. Oh, S.; Chung, K.; Ragland, D.R.; Chan, C. Analysis of wet weather related collision concentration locations: Empirical assessment of continuous risk profile. In Proceedings of the 88th Annual Meeting of the Transportation Research Board, Washington, DC, USA, 11–15 January 2009.
55. Abdel-Aty, M.; Ekram, A.-A.; Huang, H.; Choi, K. A study on crashes related to visibility obstruction due to fog and smoke. *Accid. Anal. Prev.* **2011**, *43*, 1730–1737. [CrossRef] [PubMed]
56. Aström, H.; Wallman, C. *Friction Measurement Methods and the Correlation between Road Friction and Traffic Safety: A Literature Review*; Swedish National Road and Transport Research Institute (VTI): Linköping, Sweden, 2001.
57. Lester, T. *Pedestrian Slip Resistance Testing: AS/NZS 3661.1:1993*; Opus International Consultants Ltd.: Lower Hut, New Zealand, 2014.
58. European Aviation Safety Agency. *RuFAB—Runway Friction Characteristics Measurement and Aircraft Braking: Volume 3, Functional Friction*; Research Project EASA 2008/4; BMT Fleet Technology Limited: Kanata, ON, Canada, 2010; Available online: https://easa.europa.eu/system/files/dfu/Report%20Volume%203%20-%20Functional%20friction.pdf (accessed on 5 October 2015).
59. Sarna-Wojcicki, A.M.; Shipley, S.; Waitt, R.B.; Dzurisin, D.; Wood, S.H. Areal distribution, thickness, mass, volume, and grain size of air-fall ash from the six major eruptions of 1980. In *The 1980 Eruptions of Mount Saint Helens*; USGS Numbered Series 1250; Lipman, P.W., Mullineaux, D.R., Eds.; U.S. Government Publishing Office: Washington, DC, USA, 1981; pp. 577–600.
60. Matsumoto, H.; Okabyashi, T.; Mochihara, M. Influence of eruptions from Mt. Sakurajima on the deterioration of materials. In Proceedings of the Kagoshima International Conference on Volcanoes, Kagoshima, Japan, 19–23 July 1988; pp. 732–735.
61. Delmelle, P.; Villiéras, F.; Pelletier, M. Surface area, porosity and water adsorption properties of fine volcanic ash particles. *Bull. Volcanol.* **2005**, *67*, 160–169. [CrossRef]
62. Heiken, G.; Wohletz, K. *Volcanic Ash*; University of California Press: Berkeley, CA, USA, 1985.
63. Wardman, J.B.; Wilson, T.M.; Bodger, P.S.; Cole, J.W.; Johnston, D.M. Investigating the electrical conductivity of volcanic ash and its effect on HV power systems. *Phys. Chem. Earth* **2012**, *45–46*, 128–145. [CrossRef]

64. Labadie, J.R. Volcanic Ash Effects and Mitigation. Adapted from a Report Prepared in 1983 for the Air Force Office of Scientific Research and the Defence Advanced Research Projects Agency. 1994. Available online: https://volcanoes.usgs.gov/vsc/file_mngr/file-126/Doc%209691_3rd%20ed_Appendix-A.pdf (accessed on 6 August 2017).
65. Heiken, G.; Murphy, M.; Hackett, W.; Scott, W. *Volcanic Hazards to Energy Infrastructure-Ash Fallout Hazards and Their Mitigation*; World Geothermal Congress: Florence, Italy, 1995; pp. 2795–2798.
66. Miller, T.P.; Casadevall, T.J. Volcanic ash hazards to aviation. In *Encyclopedia of Volcanoes*, 1st ed.; Sigurdsson, H., Houghton, B., Rymer, H., Stix, J., McNutt, S., Eds.; Academic Press: San Diego, CA, USA, 1999; pp. 915–930.
67. Gordon, K.D.; Cole, J.W.; Rosenberg, M.D.; Johnston, D.M. Effects of volcanic ash on computers and electronic equipment. *Nat. Hazards* **2005**, *34*, 231–262. [CrossRef]
68. Van Traffic Accident on Slippery Road, iStock Photograph 14892158, Andersen, O., 2010. Available online: http://www.istockphoto.com/photo/van-traffic-accident-on-slippery-road-gm183542417-14892158?st=a141548 (accessed on 1 February 2016).
69. Tuck, B.H.; Huskey, L.; Talbot, L. *The Economic Consequences of the 1989–1990 Mt. Redoubt Eruptions*; Institute of Social and Economic Research, University of Alaska: Anchorage, Alaska, 1992.
70. Broom, S.J. Characterisation of "Pseudo-Ash" for Quantitative Testing of Critical Infrastructure Components with a Focus on Roofing Fragility. Bachelor's Thesis, University of Canterbury, Christchurch, New Zealand, 2010.
71. Wilson, G.; Wilson, T.; Cole, J.; Oze, C. Vulnerability of laptop computers to volcanic ash and gas. *Nat. Hazards* **2012**, *63*, 711–736. [CrossRef]
72. Boyle, T. *Skid Resistance Management on the Auckland State Highway Network*; Transit New Zealand: Wellington, New Zealand, 2005. Available online: http://www.nzta.govt.nz/resources/surface-friction-conference-2005/8/docs/skid-resistance-management-auckland-state-highway-network.pdf (accessed on 15 June 2015).
73. Bastow, R.; Webb, M.; Roy, M.; Mitchell, J. *An Investigation of the Skid Resistance of Stone Mastic Asphalt Laid on a Rural English County Road Network*; Transit New Zealand: Wellington, New Zealand, 2004; pp. 1–16. Available online: http://www.nzta.govt.nz/resources/surface-friction-conference-2005/7/docs/investigation-skid-resistance-stone-mastic-asphalt-laid-rural-english-county-road-network.pdf (accessed on 16 June 2015).
74. 'Hidden Menace' on UK's Roads. *BBC News*. 2015. Available online: http://news.bbc.co.uk/2/hi/programmes/file_on_4/4278419.stm (accessed on 12 February 2015).
75. Get a Grip: Motorcycle Road Safety. *Daily Telegraph*. 2008. Available online: http://www.telegraph.co.uk/motoring/motorbikes/2750422/Motorcycle-road-safety-Get-a-grip.html (accessed on 12 February 2015).
76. NZRF (The New Zealand Roadmarkers Federation Inc.). Road Marking is Road Safety. In Proceedings of the 2005 New Zealand Road Marking Federation Inc. Conference, Christchurch, New Zealand, 17–19 August 2005; Potters Asian Pacific: Dandenong, Australia, 2005.
77. NZRF. *NZRF Roadmarking Materials Guide*; New Zealand Roadmarkers Federation Inc.: Auckland, New Zealand, 2009.
78. Downer Group. (Christchurch, New Zealand). Personal communication (by email) with roading supervisor. December 2014–January 2015.
79. ASTM International. *ASTM E303. Standard Test Method for Measuring Surface Frictional Properties Using the British Pendulum Tester*; ASTM E303-93 (Reapproved 2013); ASTM International: West Conshohocken, PA, USA, 2013.
80. TNZ (Transit New Zealand). *Standard Test Procedure for Measurement of Skid Resistance Using the British Pendulum Tester*; Report TNZ T/2:2003; Transit New Zealand: Wellington, New Zealand, 2003.
81. Hill, D.J. Filtering out the Ash: Mitigating Volcanic Ash Ingestion for Generator Sets. Master's Thesis, Hazard and Disaster Management, University of Canterbury, Christchurch, New Zealand, 2014.
82. ASTM International. *ASTM E965. Standard Test Method for Measuring Pavement Macrotexture Depth Using a Volumetric Technique*; ASTM E965-96 (Reapproved 2006); ASTM: West Conshohocken, PA, USA, 2006.
83. Kagoshima City Office (Kagoshima, Japan). Personal communication (by meeting) with road network and volcanic ash clean-up managers. 8 June 2015.